

Lawrence Berkeley National Laboratory

Recent Work

Title

NEAR-THRESHOLD FATIGUE: AN OVERVIEW OF THE ROLE OF MICROSTRUCTURE AND ENVIRONMENT

Permalink

<https://escholarship.org/uc/item/4cq2h0sq>

Author

Ritchie, R.O.

Publication Date

1984-09-01



Lawrence Berkeley Laboratory

UNIVERSITY OF CALIFORNIA

RECEIVED
LAWRENCE
BERKELEY LABORATORY

Materials & Molecular Research Division

APR 8 1985

LIBRARY AND
DOCUMENTS SECTION

Presented at the Second International Conference on Fatigue and Fatigue Thresholds, University of Birmingham, U.K., September 3-7, 1984; and to be published in the Proceedings

NEAR-THRESHOLD FATIGUE: AN OVERVIEW OF THE ROLE OF MICROSTRUCTURE AND ENVIRONMENT

R.O. Ritchie

September 1984

For Reference
Not to be taken from this room



LBL-18457
c1

DISCLAIMER

This document was prepared as an account of work sponsored by the United States Government. While this document is believed to contain correct information, neither the United States Government nor any agency thereof, nor the Regents of the University of California, nor any of their employees, makes any warranty, express or implied, or assumes any legal responsibility for the accuracy, completeness, or usefulness of any information, apparatus, product, or process disclosed, or represents that its use would not infringe privately owned rights. Reference herein to any specific commercial product, process, or service by its trade name, trademark, manufacturer, or otherwise, does not necessarily constitute or imply its endorsement, recommendation, or favoring by the United States Government or any agency thereof, or the Regents of the University of California. The views and opinions of authors expressed herein do not necessarily state or reflect those of the United States Government or any agency thereof or the Regents of the University of California.

LBL-18457

**NEAR-THRESHOLD FATIGUE: AN OVERVIEW OF
THE ROLE OF MICROSTRUCTURE AND ENVIRONMENT**

by

R. O. Ritchie

Materials and Molecular Research Division,
Lawrence Berkeley Laboratory,
and
Department of Materials Science and Mineral Engineering,
University of California, Berkeley, CA 94720, U.S.A.

September 1984

Published in "Fatigue '84," Proceedings of the Second International Conference on Fatigue and Fatigue Thresholds, C. J. Beevers, ed., EMAS Ltd., Warley, U.K., 1984.

This work was supported by the Director, Office of Energy Research, Office of Basic Energy Sciences, Materials Science Division of the U.S. Department of Energy under Contract No. DE-AC03-76SF00098.

NEAR-THRESHOLD FATIGUE: AN OVERVIEW OF THE ROLE OF MICROSTRUCTURE AND ENVIRONMENT

R. O. Ritchie*

In the four years since the First International Conference on Fatigue Thresholds held in Stockholm, interest in the topic of near-threshold fatigue, with associated small crack behaviour, has increased dramatically. In the current paper an overview is presented of the salient micro-mechanisms, primarily involving crack closure, which can influence the growth of fatigue cracks at near-threshold levels, with special emphasis on the role of microstructure and environment. Examples are drawn from recent work on crack propagation in dual-phase and low alloy steels and in under/peak/overaged aluminium alloys. Here, factors such as duplex microstructures, variations in slip mode, high pressure hydrogen environments and compression overloads are shown to modify the extent of closure, thereby causing marked changes in near-threshold crack growth behaviour.

INTRODUCTION

The existence of a limiting stress intensity range, below which fatigue cracks appear dormant, was first demonstrated by Paris in 1970 (1), although the concept had been suggested by earlier theoretical and experimental studies (2,3). Since that time, the propagation behaviour of cracks close to the fatigue threshold, ΔK_{TH} , i.e., typically below 10^{-9} m/cycle, has assumed increasing importance in fatigue research (e.g., ref. 4), with the number of technical

* Materials and Molecular Research Division, Lawrence Berkeley Laboratory, and Department of Materials Science and Mineral Engineering, University of California, Berkeley.

papers devoted to the topic rising dramatically each year (5). This appears to be due partly to the fact that it represents a relatively unexplored regime compared to the wealth of information for higher growth rates, and partly from a need for reliable engineering data for use in design and defect tolerant prediction procedures (4). However, despite its acceptance in the literature, there is an increasing body of evidence to show that fatigue threshold values for a given material can become non-unique under certain crack size, geometry and loading conditions (6). For example, it is now realized that when crack sizes are small (i.e., $\lesssim 1$ mm), as is generally the case in many service components, their behaviour may involve accelerated growth rates, even **below the threshold**, as shown schematically in Fig. 1 and reviewed recently in ref. 7. Moreover, these effects can be accentuated by environmental factors (8,9). The limiting dimensions for such non-unique behaviour appear to be where crack sizes approach the scale of the microstructure or the scale of local plasticity, or where cracks simply are physically small (i.e., $\lesssim 1$ mm) (7-10).

The importance of the small crack and near-threshold behaviour cannot be overemphasized as the lifetime of many engineering structures and components is dominated by sub-critical flaw growth in these regimes. This is well illustrated in Fig. 2 which shows actual defect tolerant fatigue lifetime predictions, in the form of defect size, a , versus life, for a Canadian sour gas pipeline (11). Although the pipeline is predicted to last in excess of 85 years,

based on the extension of an assumed 0.5 mm initial flaw to a critical crack length of 4 mm under an operational spectrum of applied loads, the first 70 years of this time is spent with the crack both smaller than 1 mm and propagating in the near-threshold regime.

In the present paper, an overview is given of the roles of microstructure and environment in influencing such near-threshold fatigue crack growth, with emphasis on the major micromechanisms which control behaviour. Experiments based on the micro-machining of material left in the wake of arrested threshold cracks clearly show fatigue crack closure to be the most dominant of these mechanisms. Examples are taken from recent studies on effects of i) duplex microstructures in dual-phase steels, ii) variations in slip mode and variable amplitude loading in aluminium alloys, and iii) high pressure hydrogen environments in pressure vessel steels.

MECHANISMS OF NEAR-THRESHOLD CRACK GROWTH

For deformation conditions of small-scale yielding where the linear elastic stress intensity factor, K_I , provides an asymptotic characterisation of crack tip stress and strain fields, it is now well established for cyclic loading that the rate of growth of fatigue cracks, da/dN , can be correlated with stress intensity range, ΔK , given by the difference between the maximum and minimum stress intensities per cycle and computed globally in terms of geometry and applied loads (12):

$$\Delta K = K_{\max} - K_{\min} \quad (1)$$

However, the local driving force experienced at the crack tip may differ from the nominal (far field) ΔK where factors such as cyclic plasticity, crack deflection and closure perturb the near-tip field. Of these, crack closure and to a lesser extent deflection are most relevant at near-threshold levels since the spread of local plasticity is limited to the extent that invariably plane strain conditions prevail with crack tip opening displacements (CTOD) and plastic zone sizes both small compared to microstructural size-scales.

Crack Closure

Plasticity-induced closure. Fatigue crack closure, as originally described by Elber (13), was considered to arise from the elastic constraint, of material surrounding the plastic zone enclave in the wake of the crack tip, on material elements previously plastically stretched at the tip. The resulting interference between crack surfaces, which clearly predominates at low load ratios, can lead to a reduction in crack driving force from the nominal ΔK value to some lower effective value, ΔK_{eff} , actually experienced at the tip, viz:

$$\Delta K_{\text{eff}} = K_{\max} - K_{c1} \quad (2)$$

where K_{c1} is the closure stress intensity representing the point of first contact between the crack surfaces during unloading. Closure

arising from cyclic plasticity, generally referred to as **plasticity-induced closure**, is most prevalent under plane stress conditions (14), and thus is more significant at higher stress intensities, rather than at near-threshold levels.

At the ultra-low growth rates associated with near-threshold levels, several other sources of closure have been shown recently to assume greater importance (15). As schematically illustrated in Fig. 3, these mechanisms involve the wedging action of crack flank corrosion deposits (16-18) and fracture surface asperities (18-21), coupled with significant crack tip shear displacements (22), fluid-induced pressure between the crack walls (23-25), and compression between the crack surfaces resulting from certain metallurgical phase transformations (15). Since a detailed description of these alternative closure mechanisms has been the subject of a recent review (15), only a brief summary is presented here.

Oxide-induced closure. Crack closure arising from crack surface corrosion deposits, generally referred to as **oxide-induced closure**, is promoted in moist, oxidizing environments when the size-scale of the debris becomes comparable with crack tip opening displacements (18). Notable examples are the crack surface oxides and calcareous deposits formed during corrosion fatigue in structural steels tested, respectively, in water and seawater (26,27), and the chromic oxides formed during creep-fatigue in Ni-based superalloys (28). Simple quantitative modelling, based on the concept of a rigid wedge inside a linear elastic crack, suggests that the closure which results from

such deposits depends upon the thickness of the oxide film, s , the location of its peak thickness from the crack tip, 2ℓ , Poisson's ratio, ν , and Young's modulus, E , i.e. (29):

$$K_{c1} \approx \frac{s E}{4\sqrt{\pi\ell} (1 - \nu^2)} \quad (3)$$

This relationship clearly shows that deposits in the immediate vicinity of the crack tip will have a dominating influence in the development of closure by this mechanism (30).

In lower strength materials, particularly in low carbon steels, the extent of the corrosion debris can be significantly enhanced at **low load ratios** from fretting oxidation processes (31) between the crack walls, leading to a greater accumulation of deposits and hence to more closure (16-18,27-30). This can produce surprising results, such as observations in lower strength alloy steels of near-threshold growth rates at $R = 0.05$ being significantly faster in dry helium gas (18), and slower in water or steam (27), compared to behaviour in room air. Since susceptibility to hydrogen embrittlement is not large in these steels, at the high frequencies and low growth rates characteristic of near-threshold conditions, such results simply can be interpreted in terms of less corrosion deposits being generated in the dry atmosphere and more in the wet environment, thereby governing the extent of oxide-induced closure (18). With steels of higher tensile strength (32,33) and in the majority of aluminium alloys (34-38), the degree of fretting oxidation between crack surfaces appears much reduced, with the result that, except in very oxidizing

environments (27), the thickness of the fracture surface oxide films remains small compared to the crack opening displacements such that the contribution to closure from this mechanism becomes negligible (15).

Roughness-induced closure. A more general source of crack closure, which is especially important in precipitation hardened (36-38) and dual phase (39,40) microstructures, arises from the wedging action of fracture surface asperities, where crack tip opening displacements are small and where significant Mode II crack tip shear displacements occur (19-21). Such **roughness-induced closure** thus is promoted at near-threshold levels, particularly since crack advance in this regime tends to occur via a single shear type mechanism (i.e., involving Mode II + I displacements akin to Forsyth's Stage I (41)) when the extent of crack tip plasticity does not exceed the characteristic microstructural dimensions. This induces a faceted or crystallographic mode of crack growth (Fig. 4), which is most prevalent in coherent particle hardened (planar slip) systems (e.g., underaged aluminium alloys (36-38) and Ni-based superalloys (42,43)), thereby enhancing closure from increased asperity contact (Fig. 5). Significant roughness-induced closure also can be generated in certain duplex microstructures where crack paths can be made to meander from frequent crack deflection (45) at the harder phase (e.g., in ferritic-martensitic dual-phase steels (39,40) and β -annealed titanium alloys (46,47)).

The magnitude of the contribution from the roughness-induced mechanism appears to depend upon the degree of fracture surface roughness and the extent of the Mode II crack tip displacements. For example, from simple two-dimensional geometric modelling of the process, the non-dimensional closure stress intensity at the point of first asperity contact has been derived to be (21):

$$K_{c1} \approx \sqrt{\frac{2\gamma u}{1 + 2\gamma u}} \cdot K_{\max} \quad , \quad (4)$$

where γ is the measure of surface roughness taken as the ratio of height to width of the asperities and u is the ratio of Mode II to Mode I crack tip displacements. Although only a first-order model, experimental results in a range of ferrous and non-ferrous alloys have been found to be in reasonable agreement with this relationship (40,43,49).

Fluid-induced closure. Crack closure also can be generated in liquid environments through the hydrodynamic action of fluid within the crack. Such fluids can generate an internal fluid pressure, which acts to oppose the closing, and to a lesser extent the opening, of the crack under cyclic loading (23-25). The magnitude of this internal pressure distribution, $p(x)$, shown schematically in Fig. 6, is a function of several factors, including the absolute viscosity of the fluid, η_0 , the magnitude of crack opening, h , the closing velocity of the crack walls, $\dot{\theta}$, and most importantly the degree of fluid penetration, d , into the crack. Thus, for a fatigue crack of length a , where the pressure $p(x)$ at distance x from the crack mouth

is given by (25):

$$p(x) = \frac{6npa^3}{h_m^3} \log[1 - (x/a)]\dot{\theta}, \quad d/a = 1, \quad (5a)$$

or

$$p(x) = 6np \frac{\langle \dot{h} \rangle}{\langle h \rangle^3} x(d - x), \quad d/a < 1, \quad (5b)$$

and where the extent of fluid penetration, d , can be assessed from capillary flow arguments, in terms of the fluid surface tension, γ_L , and wetting angle, β , as (25):

$$d^2(t) = \left(\frac{\gamma_L \cos \beta}{3np} \right) \int_0^t \langle h \rangle (t) dt, \quad (6)$$

estimates of the "effective" closure stress intensity, K_{\max}^* can be computed and superimposed onto the applied stress intensities to derive the variation in ΔK_{eff} (Fig. 7). Predicted values for a 2.25Cr-1Mo pressure vessel steel, fatigued at a nominal ΔK of $10 \text{ MPa}\sqrt{\text{m}}$ ($R = 0.05$) in oils of varying viscosity, are shown as a function of penetration distance in Fig. 8 and crack length in Fig. 9 (25). It is apparent from Figs. 7 and 8 that the closure effect is comprised of two parts: the fluid opposes both the closing of the crack, which gives an effective increase in K_{\min} by an amount K_p , and the opening of the crack, which gives a smaller effective decrease in K_{\max} by an amount K_q , where

$$K_{\max}^* = K_q + K_p. \quad (7)$$

The magnitude of the closure effect also can be seen to be decreased

with decreasing crack length (Fig. 9), consistent with current ideas on the role of closure in influencing the growth of short cracks (7).

In general, fluid-induced closure should be promoted in higher viscosity liquids, but the development of a fluid pressure quickly saturates (Figs. 8 and 9) and further is offset by the slower penetration kinetics of highly viscous fluids into the crack. The maximum contribution to closure from this mechanism should be such that $K_{\max}^* \rightarrow K_{\max}$ (i.e., $\Delta K_{\text{eff}} \rightarrow 0$) as $\eta \rightarrow \infty$. However, for the majority of viscous fluids (i.e., $\eta < 10^5$ cS), values of K_{\max}^* tend to saturate close to the mean stress intensity in the cycle, due to the minimal changes in K_q , such that the maximum extent of closure is generally of the order of K_{c1}/K_{\max} of 0.5 (25). Thus, the hydrodynamic wedge mechanism must be regarded as a less potent mechanism of closure, compared to that generated by cyclic plasticity, corrosion deposits and fracture surface asperities, where considerably larger values of K_{c1}/K_{\max} are possible.

Other mechanisms of closure. Reductions in the local crack driving force due to closure can arise through various other mechanisms, such as the presence of residual stresses in a structure or the occurrence of a stress- or strain-induced phase transformation in the vicinity of the crack tip (15). In the latter case, austenite-to-martensite transformations in, say, austenitic stainless steels involve a positive volume change of typically 4% and, due to the constraint of surrounding elastic material, regions of transformed material will be placed under compression. Once the

crack penetrates such regions, generally corresponding to some crack tip process zone, the compressive stresses act to close the crack, thereby reducing the nominal stress intensity to some lower effective value. No quantitative models currently exist for this closure mechanism, although solutions are available for the analogous situation of stress-induced dilatant transformations under monotonic loading (49).

Crack-Deflection

As recently described by Suresh (45), near-threshold fatigue crack growth behaviour also can be influenced markedly by the process of crack deflection. Although Mode I da/dN data invariably are analysed assuming a linear crack orientated perpendicular to the plane of maximum tensile stress, cracks frequently deviate from this path due to load excursions, environmental effects or interaction with specific microstructural features. The result of such deflection, whether associated with a simple kink, twist or more complex bifurcation, is a reduction in the local Mode I driving force (45). For example, two-dimensional linear elastic analysis for a crack subjected to both shear and tensile loads which undergoes a simple kink at angle θ to the crack plane, gives solutions for the local Mode I and Mode II stress intensities at the tip of the deflected crack, k_1 and k_2 , in terms of the nominal stress intensities, K_I and K_{II} and angular functions $a_{ij}(\theta)$ as (50):

$$\begin{aligned} k_1 &= a_{11}(\theta)K_I + a_{12}(\theta)K_{II} \quad , \\ k_2 &= a_{21}(\theta)K_I + a_{22}(\theta)K_{II} \quad , \end{aligned} \quad (8)$$

such that the effective near-tip driving force can be considered as:

$$k_{\text{eff}} = (k_1^2 + k_2^2)^{\frac{1}{2}} \quad . \quad (9)$$

For a simple 45° deflected crack, where the length of the branch is small compared to the crack length, solutions to Eqs. (8) and (9) suggest roughly a 20% reduction in local Mode I stress intensity factor resulting from the deflection (45).

The effect of crack deflection is several fold. Not only is the local Mode I crack driving force reduced and the length of crack path increased, but the resultant Mode II shear promotes roughness-induced crack closure under cyclic loading conditions (21). Accordingly, microstructures which enhance tortuosity in crack path generally show excellent resistance to near-threshold crack growth. As discussed below, coherent particle hardened and duplex microstructures are notable examples in this regard.

ROLE OF ENVIRONMENT

The role of environment in influencing rates of fatigue crack growth at near-threshold levels in general is extremely complex due to the many environmentally-induced contributions to both the mechanical and chemical crack driving force. This topic has been reviewed recently for the advance of both short and long cracks at low growth rates in refs. 9 and 51, respectively. Specifically,

environmentally-affected crack extension at near-threshold stress intensities often must be considered in terms of the mutual competition of two concurrent mechanisms; namely the acceleration in growth rates due to the contribution from corrosion fatigue mechanisms, such as hydrogen embrittlement or active path corrosion, must be offset by the deceleration in growth rates caused by a resultant increase in closure. Such enhanced closure due to environmental effects can take several forms, such as an increase in the contribution from the oxide-induced mechanism arising from the products of the crack tip electrochemical reaction, increases in roughness-induced closure from changes in crack path morphology, or the development of fluid-induced closure from the presence of a liquid medium within the crack (e.g., 15-18,24,52).

Where such closure effects dominate, such as during near-threshold growth in lower strength coarse-grained alloys at low load ratios, observed environmental effects may be markedly different from well-documented corrosion fatigue results for higher growth rates (51). For example, it is well known that fatigue crack propagation rates in lower strength steels above $\sim 10^{-8}$ m/cycle are **slower** in the presence of gaseous helium and **faster** in water environments, compared to room air, due to the suppression or enhancement, respectively, in the contribution to cracking from hydrogen embrittlement and/or metal dissolution mechanisms. At near-threshold growth rates, however, where the effect of such corrosion fatigue mechanisms is much reduced (due in part to the high frequencies utilised in near-threshold

testing), growth rates are **faster** in helium gas and **slower** in water, simply because the wet environments promote oxide-induced closure whereas the dry environments suppress it (15-18,53). Such differences are not observed at high load ratios where the influence of crack closure is much diminished from the larger crack opening displacements.

Role of Prolonged Hydrogen Exposure

Another example of the offsetting influences of environmentally-induced damage and crack closure can be seen in recent studies on the role of hydrogen attack in influencing fatigue crack growth rates in pressure vessel steels (54). Prior exposure of low alloy steels, such as the Mn-Ni-Mo ASTM A533B nuclear pressure vessel steel, to high pressure (~ 17 MPa) gaseous hydrogen at high temperatures ($\sim 600^\circ\text{C}$) for prolonged periods of time (~ 1000 hr) can lead to the formation, on prior austenite grain boundaries, of internal bubbles of methane gas from the reaction between ingressed hydrogen and carbides in the steel (termed hydrogen attack). For cases of severe attack (SA), where bubbles start to coalesce to form larger fissures, the effect on mechanical properties can be devastating: reductions in yield strengths typically by factors of 3 to 4 commonly are seen due to the accompanying decarburization, together with losses in ductility (%RA) and toughness (K_{IC} and upper shelf Charpy impact energy), by factors of ~ 10 to 15 (since the voids act as ready

nucleation sites for fracture by microvoid coalescence).^{*} What is surprising, however, is when such severely attacked structures are tested in fatigue and compared with lightly attacked (LA) and unattacked (heat treated, HT) structures, the effect of the damage is relatively insignificant at near-threshold levels, although there is some acceleration in growth rates above 10^{-8} m/cycle (Fig. 10) (54).

The reason for the minimal effect close to ΔK_{TH} can be appreciated with reference to Figs. 11 and 12. Severe hydrogen attack damage in the form of extensive grain boundary void formation gives rise to a cavitated intergranular fracture mode during fatigue crack growth, which results in an extremely tortuous crack path compared to the almost linear profiles of crack paths in unattacked microstructures (Fig. 11). Coupled with the associated softening from decarburisation, the generation of such rough fracture surfaces leads to a significant increase in the magnitude of the crack closure in severely attacked structures, as shown by the experimental back-face strain measurements of K_{c1}/K_{max} in Fig. 12 (54).

Thus, microstructural damage from grain boundary void formation following prolonged exposure to high temperature, high pressure hydrogen environments, which causes severe degradations in strength, ductility and toughness properties, has only a marginal effect on the propagation of fatigue cracks at near-threshold levels since any

*Plane strain fracture toughness, K_{IC} , values, computed from J_{IC} measurements, show a dramatic decrease from $180 \text{ MPa}\sqrt{\text{m}}$ in the unattacked condition to a mere $20 \text{ MPa}\sqrt{\text{m}}$ after severe hydrogen attack.

acceleration in growth rates due to hydrogen attack damage is offset by a local reduction in crack driving force from the concomitant increase in crack closure.

ROLE OF MICROSTRUCTURE

Similar to the role of environment described above, many of the microstructural effects observed for fatigue crack propagation at near-threshold levels can be linked to a prominent role of crack closure, particularly since they are accentuated at low load ratios. Of these effects, the principal microstructural variables affecting closure and low growth rate behaviour appear to be grain size, precipitate type and distribution, slip characteristics and, in duplex structures, the proportion and morphology of the two phases. In many instances, optimising these variables for maximum near-threshold fatigue resistance can have the opposite effect on other mechanical properties, such as toughness, ductility and resistance to fatigue crack initiation. For instance, microstructures with increasing grain sizes invariably show the highest ΔK_{TH} values yet this generally reduces fracture toughness and the initiation-controlled fatigue limit (55). Similarly, coherent particle hardening, which induces planar slip, is beneficial for near-threshold fatigue resistance as it leads to crystallographic crack paths which promote crack deflection and roughness-induced closure, yet the resulting strain localisation can be very detrimental to both ductility and toughness (38). Near-threshold fatigue crack

propagation behaviour in dual-phase steels and in precipitation hardened aluminium alloys provides illustrative examples of these effects, as discussed below.

Behaviour in Duplex Microstructures

Ferritic-martensitic dual-phase steels provide an excellent metallurgical system to improve near-threshold fatigue crack growth resistance through the generation of tortuous crack paths by crack deflection at interfaces, leading to enhanced roughness-induced closure (39,40,56,57). Recent studies on duplex microstructures in Fe-2Si-0.1C (40) and plain carbon AISI 1008 to 1020 (39,56,57) steels have shown that by modifying the proportion and primarily the morphology of the ferrite and martensite phases through intercritical heat treatment, increases in the ΔK_{TH} value by up to a factor of two can be readily obtained **without loss in strength** (Fig. 13). Such marked increases in crack growth resistance, shown in Figs. 13 and 14 specifically for step quenched (SQ) and intercritical annealed (IA) structures in Fe-2Si-0.1C, are associated with measured increases in closure and can be attributed to the production of meandering crack paths from frequent deflection at ferrite-ferrite and ferrite-martensite interfaces (Fig. 14) (40,45).

As stated above, the benefits of such crack paths are to reduce the local crack driving force from both crack deflection mechanics and from roughness-induced closure. In Fig. 15, an attempt is made to separate the contribution from these two mechanisms, for the dual-

phase steel results shown in Fig. 13 (40). The raw da/dN vs. ΔK data first are plotted against ΔK_{eff} by incorporating measured K_{c1} values (Fig. 15a). The differences in da/dN which remain between the microstructures (Fig. 15b), which now are independent of closure, are then rationalised in terms of two-dimensional elastic crack deflection models (45), using estimates of the extent of crack deviation from Fig. 14. It is apparent from such approximate analyses that, in the present duplex microstructures, the superior crack growth resistance from the generation of meandering crack paths can be attributed to roughness-induced crack closure and crack deflection, with specific contributions in the ratio of roughly 2:1 (40).

As pointed out several years ago by McEvily (39), the benefits of this approach in dual-phase steels are that very high thresholds can be obtained without lowering tensile strength. In fact, in the intercritical annealed Fe-2Si-0.1C steel, the ΔK_{TH} value of almost $20 \text{ MPa}\sqrt{\text{m}}$, with a yield strength of 600 MPa, is believed to represent the highest ambient temperature threshold ever reported and certainly represents the highest combination of fatigue threshold and yield strength measured to date in ferrous alloys (Fig. 16) (40).

Behaviour in Precipitation Hardening Systems

Similar enhancements in near-threshold fatigue crack propagation resistance through the deflection of the crack path can be achieved by modifying the nature of the slip mode in precipitation hardening

alloys. In aluminium alloys, for example, underaged microstructures generally show higher thresholds and lower near-threshold growth rates than peak and overaged microstructures, as shown for I/M 7150 alloy in Fig. 17 (38). Such differences are reduced at high load ratios and are virtually non-existent at higher growth rates above 10^{-9} m/cycle. The increasing resistance to near-threshold crack growth with decreased ageing once more can be associated with a measured increase in crack closure and attributable mechanistically to a greater propensity for crack path deviation, and hence in rougher fracture surfaces, in the lightly aged structures (Fig. 18) (35-38). This follows because underaged microstructures are hardened primarily by the shearing of small coherent precipitates resulting in heterogeneous deformation (i.e., planar slip), which promotes crystallographic crack paths (58). The added benefit of such a deformation mode is that slip at the crack tip is occurring on fewer slip systems, thereby raising the degree of slip reversibility which lessens the crack tip damage per cycle (58,59). Conversely, in more heavily aged systems where the mode of hardening becomes one of Orowan bypassing around larger semi-coherent or incoherent (non-shearable) precipitates, the resulting homogeneous deformation (i.e., wavy slip) generates a far more planar fracture surface due to the larger number of finer slip steps. This leads to less roughness-induced closure and less slip reversibility resulting in more crack tip damage per cycle.

As mentioned above, such microstructural factors, which provide increased fatigue crack growth resistance at near-threshold levels, actually may be detrimental to other mechanical properties. For example, the planar slip characteristics of coherent particle hardened microstructures, which are so potent in generating superior fatigue properties, can lead simultaneously to inferior fracture toughness from a greater tendency for strain localisation (38). This is particularly evident in aluminium-lithium alloys where the increased coherency between lithium-containing intermetallics and the matrix can result in exceptionally good fatigue crack propagation resistance, through enhanced crack path tortuosity, yet at the same time can produce extremely low toughness values (60).

LOCATION OF CRACK CLOSURE AND THE THRESHOLD CONDITION

Since crack closure is clearly crack size and load history dependent, doubts have been expressed over the uniqueness of near-threshold data in terms of the differing loading paths incorporated into the various experimental procedures used to approach the threshold (e.g., 61,62). Several studies, for example, have shown an influence of the rate of load shedding on the value of ΔK_{TH} (63), although in general the effect is not that large. The crucial factor here is where the prominent location of the closure is in relation to the crack tip. If the major closure effect is within, say, $\sim 500 \mu\text{m}$ of the tip, it is likely to affect subsequent crack growth over further extensions of that order. Conversely, if closure

predominates over distances far behind the tip (i.e., \sim several mm), a significant influence of prior loading history (e.g., of dK/da) is to be expected.

Experiments to Remove Closure

Several recent studies on near-threshold fatigue crack growth have been directed at identifying the most prominent locations of such closure in relation to the crack tip, and furthermore in defining more precisely how crack closure itself can control the fatigue threshold condition (64-69). One promising experimental approach has been to monitor the behaviour of cracks, arrested at ΔK_{TH} , both during and following the physical removal of closure forces along the crack length. This has been achieved principally through the micro-machining of material left in the wake of the crack tip (65-69) and through the application of large single compression overloads (70-73).

Crack tip wake removal. Experiments, where mechanical or electro-discharge machined slots (of width < 0.5 mm) have been used to remove the wake of arrested threshold cracks in both steels and aluminium alloys (65-69), indicate that the majority of the closure is located in the immediate vicinity of the crack tip. For example, Fig. 19 shows the variation, in several microstructures in 7150 aluminium, of K_{c1}/K_{max} values along the length of a threshold crack, monitored *in situ* using back-face strain measurements at each machining increment (68). Although the closure at $R = 0.10$ is

distributed reasonably evenly along most of the crack length, more than 50% is confined to within 500 μm of the crack tip. No changes could be detected at $R = 0.75$.

The effect of this reduction in closure following micro-machining of the crack tip wake material from arrested threshold cracks is readily apparent by re-cycling at a constant stress intensity range of $\Delta K = \Delta K_{TH}$ (66-68). As shown in Figs. 20 and 21 for under-, peak and overaged 7150 aluminium alloys, threshold cracks at $R = 0.10$ re-commence to propagate following wake removal, consistent with their locally increased ΔK_{eff} values. However, since crack closure is found to re-develop with crack extension, to approach ~ 70 to 80% of previous (pre-machining) levels, subsequent crack extension occurs under progressively decreasing growth rates until the crack almost re-arrests (68). As the principal contribution to closure in precipitation hardened alloys is from the roughness-induced mechanism (see above), post-machining crack growth rates in the underaged structure decelerate over smaller extensions (i.e., $\sim 20 \mu\text{m}$) than in the more heavily aged structures (i.e., ~ 50 to $100 \mu\text{m}$), due to a more deflected (crystallographic) crack path (Fig. 18). At high load ratios, however, where closure effects become minimal, arrested threshold cracks remained dormant following identical wake removal procedures (Fig. 20).

Such experiments also represent the growth of short crack emanating from notches (c.f., Fig. 21 with Fig. 1). Although not performed on naturally-occurring small cracks, the results indicate

that physically short cracks, possessing a limited wake, are subjected to a smaller influence of closure, which contributes to their ability to propagate at nominal stress intensities at or below the fatigue threshold, often at progressively decreasing speeds (68). As shown in Fig. 21, growth rates become non-unique with stress intensity range because behaviour is controlled by a ΔK_{eff} value which must reflect the offsetting effects of an increase in crack length and an increase in closure.

Compression overloads. Similar observations of the re-initiation of arrested threshold cracks at ΔK_{TH} due to the physical removal of closure have been obtained through the application of single (spike) compression overloads (70,71). This is illustrated in Fig. 22 for under-, peak and overaged 7150 aluminium following the application of single 500% compression cycles (i.e., a compression load of 5 times the maximum tensile load in the fatigue cycle) (70). As with behaviour following wake removal (Fig. 20), threshold cracks at low load ratios are seen to re-commence to propagate, even though the stress intensity range does not exceed ΔK_{TH} , consistent with a measured decrease in closure. At high load ratios, conversely, threshold cracks remain dormant following either compression overloads or tensile underloads, consistent with no detectable changes in closure. Subsequent propagation at low R again involves re-development of closure with crack extension causing post-overload growth rates to progressively decrease until re-arrest (70,71). The resulting variations in ΔK_{eff} , computed from experimental K_{c1}

measurements before and after the compression cycle, are shown in Fig. 23. As before, the crack extension necessary for re-arrest is shortest in the underaged microstructure, due to its greater efficiency in generating closure from a tortuous crack path (70).

The origin of the reduction in closure following the compression cycle at ΔK_{TH} is thought to arise from two factors. First, a compression cycle reduces the magnitude of the residual compressive stress within the cyclic plastic zone at the crack tip, to a degree dependent upon the relative magnitudes of the applied compressive stress and the yield stress in compression, thereby lowering the opening load on the next cycle (72,73). Second, fractographic studies clearly suggest a reduction in roughness-induced closure from severe abrasion between post-overload fracture surfaces (70). This is shown in Fig. 24 for the underaged 7150 alloy, where compared to the distinct features of the faceted fracture surface before the compression overload (Fig. 24a), post-overload surfaces show frequent evidence of compacted fretting oxide debris (Fig. 24b) and the crushing and cracking of fracture surface asperities (Fig. 24c,d).

These experiments clearly indicate that the existence of a measured threshold stress intensity range for the advance of long fatigue cracks is controlled primarily by the level of closure. This does not imply that all cracks must remain dormant when $\Delta K = \Delta K_{TH}$ since the nominal stress intensity range at the threshold is defined independent of closure. Thus, reduction in crack size or the application of overload cycles, for example, which markedly affect

closure loads, will lead to instances of crack extension at or below ΔK_{TH} . However, since the majority of such closure appears to be located within the immediate vicinity of the crack tip, the variations in measured threshold values with loading history, specifically with rate of decrease in ΔK to approach ΔK_{TH} , are not as large as might be expected.

SUMMARY AND CONCLUDING REMARKS

In this overview, an attempt has been made to highlight the major characteristics of the fatigue threshold and near-threshold fatigue crack growth, with emphasis on the role of microstructure and environment. It is apparent that fatigue crack closure in particular plays a dominant role in dictating behaviour in this ultra-low growth rate regime, whether originating from cyclic plasticity, corrosion debris, fracture surface asperities, or from other phenomena.

From a fundamental viewpoint, the description of near-threshold behaviour in the mechanistic terms of closure, and crack deviation, has provided an excellent rationalisation of the majority of experimental observations. It also has been important in the development of microstructures with vastly improved resistance to crack extension, principally through the enhancement of closure forces. Improved interpretations of the effects of variable amplitude loading on fatigue crack growth (74) have resulted from a consideration of these factors, and they may provide the critical

link needed to unify the classical stress/strain-life and defect tolerant (long crack da/dN) analyses of fatigue (6).

Several problem areas remain, however. Firstly, quantitative models for the various closure mechanisms are still largely first order and, in general, fail to predict the influence of crack size on K_{C1} which is so critical to the description of the small crack problem (e.g., 21,29,75-77). Secondly, experimental techniques to measure such closure have not as yet been standardised, and further there is little understanding of the relationship between the microscopic aspects of very near-tip closure and the macroscopic changes, e.g., elastic compliance, used to characterise it. Thirdly, the role of geometry (78) and, most importantly, crack size still remain major areas for future research, although much progress has been made with the latter topic in recent years (reviewed in refs. 7 and 9). Of real significance here is not only the modelling of the limitation in closure forces at short crack sizes but the lack of a field parameter to either globally or locally characterise the stress and deformation fields around small cracks, since currently accepted mechanics descriptions based on K_I or J in many instances become invalidated (79).

From an engineering prediction and design perspective, the benefits of a fundamental description of fatigue thresholds are less obvious. In fact, there clearly is some inherent danger in utilising low load ratio thresholds in engineering (defect tolerant) design to predict the absence of fatigue cracking. This follows because the

threshold conventionally is defined in terms of a **nominal** stress intensity range below which a **long** crack will not propagate. Aside from the fact that it is the small cracks that generally are encountered in service, mechanisms such as crack closure and crack deflection act to vary the **local**, and not the nominal (or global), driving force. In this regard, they serve to promote the invalidity of the fracture mechanics similitude concept whereby cracks of differing lengths, subjected to the same nominal driving force, are assumed to extend at equal rates (79); a concept which currently forms the basis of scaling of laboratory data to predict component life.

Although such scaling has been established for long fatigue and statically-loaded cracks extending at higher growth rates in essentially benign environments, stress intensity-based similitude must also be modified to account for several phenomena, which at near-threshold levels largely pertain to changes in closure. Thus, wherever the extent of closure is restricted, such as at high load ratios, with small flaws or cracks at notches, or in the presence of large compressive stresses, the consequent increase in near-tip driving force will lead to accelerated growth rate behaviour and, most significantly, **to crack advance at ΔK levels at or below the ΔK_{TH} threshold**. For this reason, the use of fatigue thresholds in engineering design must be considered with extreme care.

ACKNOWLEDGMENTS

This work was supported primarily by the Director, Office of Energy Research, Office of Basic Energy Sciences, Materials Science Division of the U.S. Department of Energy under Contract No. DE-AC03-76SF00098. In addition, the studies on 7150 aluminium were supported by the U.S. Air Force Office of Scientific Research and the research on hydrogen attack by the Advanced Research and Development Fossil Energy Materials Program of the Department of Energy. Thanks are due to my former student, Dr. S. Suresh, who performed all of our early work on closure, to my colleagues, Drs. A. G. Evans, G. Thomas and W. Yu, for many helpful discussions, to my current students, R. D. Pendse, J.-L. Tzou and E. Zaiken for access to their as yet unpublished results and to Madeleine Penton for help in preparing the manuscript.

SYMBOLS USED

- a = total crack length
- $a_{ij}(\theta)$ = angular functions in Eq. (8)
- \tilde{a} = length of fatigue crack from notch
- \tilde{a}_{TH} = value of \tilde{a} at ΔK_{TH}
- Δa = crack extension following overload
- b = uncracked ligament
- B = specimen thickness
- d = penetration distance of fluid inside crack
- d_g = grain size

da/dN = fatigue crack growth rate per cycle
 D = length of deflected segment of tilted crack
 E = elastic (Young's) modulus
 $h_m, \langle h \rangle$ = maximum and average crack width, respectively
 J = J-contour crack tip integral
 k_1, k_2 = local Mode I and Mode II stress intensities
 k_{eff} = effective local stress intensity
 K_I, K_{II} = nominal Mode I and Mode II stress intensities
 K_{Ic} = plane strain fracture toughness (in Mode I)
 K_{c1} = closure stress intensity
 K_{max} = maximum stress intensity in fatigue cycle
 K_{min} = minimum stress intensity in fatigue cycle
 K_{max}^* = maximum stress intensity due to fluid pressure
 K_p = increase in K_{min} due to fluid pressure
 K_q = decrease in K_{max} due to fluid pressure
 ΔK = nominal stress intensity range ($K_{max} - K_{min}$)
 ΔK_{eff} = effective stress intensity range ($K_{max} - K_{c1}$)
 ΔK_{TH} = fatigue threshold stress intensity range
 ℓ = half distance to crack tip of peak oxide
 $p(x)$ = fluid-induced pressure along crack length
 r_y = cyclic plastic zone size
 R = load ratio (K_{min}/K_{max})
 s = peak oxide thickness
 S = length of straight segment of tilted crack
 t = time

u = ratio of Mode II to Mode I displacements
 x = length coordinate along crack
 β = wetting angle
 γ = asperity height-to-width ratio
 γ_L = surface tension
 η = kinematic viscosity
 ν = Poisson's ratio
 ρ = density of fluid
 σ_y = yield strength
 θ = angle of deflection from crack plane
 $\dot{\theta}$ = angular closing velocity of crack walls

REFERENCES

1. Paris, P. C., 1970, Closed Loop Magazine, 2, 11
2. McClintock, F. A., 1963, in Fracture of Solids, Interscience, New York, p. 65
3. Frost, N. E., 1966, in Proc. First Int. Conf. on Fracture, T. Yokobori, eds., Sendai, Japan, p. 1433
4. Ritchie, R. O., 1979, Int. Met. Rev., 20, 205
5. Taylor, D., 1984, in Fatigue '84, Proc. Second Int. Conf. on Fatigue and Fatigue Thresholds, C. J. Beevers, ed., EMAS Ltd., Warley, vol. 1, p. 327
6. Ritchie, R. O., 1984, in Proc. Sixth Int. Conf. on Fracture (ICF-6), S. R. Valluri, ed., Pergamon Press, Oxford, England.
7. Suresh, S., and Ritchie, R. O., 1984, Int. Met. Rev., 29, 445
8. Gangloff, R. P., 1981, Res. Mech. Let., 1, 299
9. Gangloff, R. P., and Ritchie, R. O., 1984, in Fundamentals of Deformation and Fracture, Proc. Eshelby Memorial Symp., B. A. Bilby and K. J. Miller, eds., Cambridge University Press.
10. Lankford, J., 1984, Fat. Eng. Mat. Struct., 7, in press
11. Vosikovsky, O., and Cooke, R. J., 1978, Int. J. Press. Ves. Piping, 6, 113
12. Paris, P. C., and Erdogan, F., 1963, J. Bas. Eng., Trans. ASME Ser. D, 85, 528
13. Elber, W., 1970, Eng. Fract. Mech., 2, 37
14. Lindley, T. C., and Richards, C. E., 1974, Mater. Sci. Eng., 14, 281

15. Suresh, S., and Ritchie, R. O., 1984, in Fatigue Crack Growth Threshold Concepts, D. L. Davidson and S. Suresh, eds., TMS-AIME, Warrendale, p. 227
16. Ritchie, R. O., Suresh, S., and Moss, C. M., 1980, J. Eng. Matl. Tech., Trans. ASME Ser. H. 102, 293
17. Stewart, A. T., 1980, Eng. Fract. Mech., 13, 463
18. Suresh, S., Zamiski, G. F., and Ritchie, R. O., 1981, Metall. Trans., 12A, 1435
19. Walker, N., and Beevers, C. J., 1979, Fat. Eng. Mat. Struct., 15, 633
20. Minakawa, K., and McEvily, A. J., 1981, Scripta Met., 15, 633
21. Suresh, S., and Ritchie, R. O., 1982, Metall. Trans., 13A, 1627
22. Davidson, D. L., 1981, Fat. Eng. Mat. Struct., 3, 229
23. Endo, K., Okada, T., Komai, K., and Kiyota, M., 1972, Bull. JSME, 15, 1316
24. Tzou, J.-L., Suresh, S., and Ritchie, R. O., 1985, Acta Met., 33, 105
25. Tzou, J.-L., Hsueh, C. H., Evans, A. G., and Ritchie, R. O., 1985, Acta Met., 33, 117
26. Scott, P. M., Thorpe, T. W., and Silvester, D. R. V., 1983, Corr. Sci., 23, 559
27. Suresh, S., and Ritchie, R. O., 1983, Eng. Fract. Mech., 18, 785
28. Yuen, J. L., Roy, P., and Nix, W. D., 1984, Metall. Trans., 15A, 1769

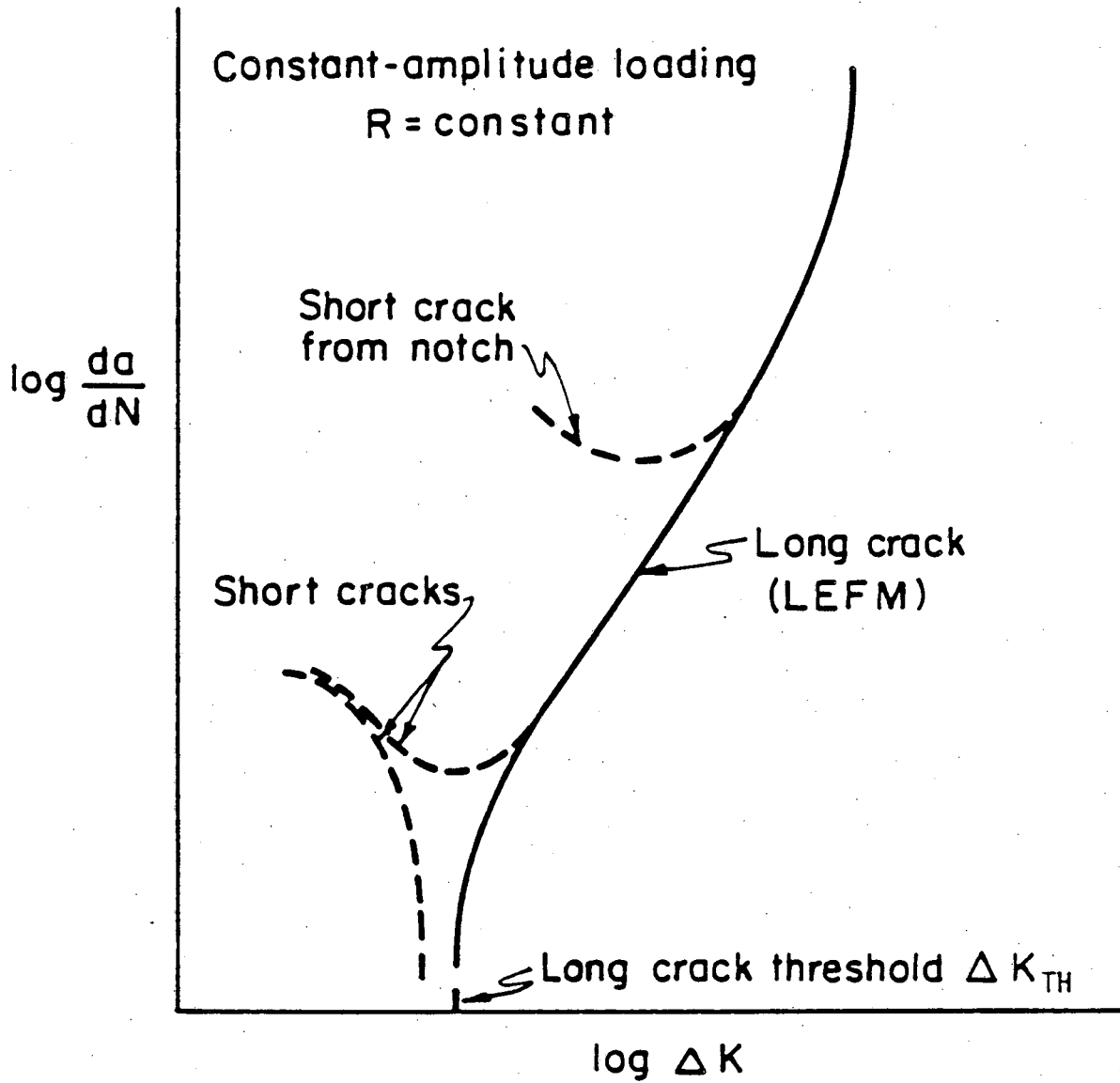
29. Suresh, S., Parks, D. M., and Ritchie, R. O., 1982, in Fatigue Thresholds, Proc. First Int. Conf. on Fatigue Thresholds, J. Bäcklund, A. Blom, and C. J. Beevers, eds., EMAS Ltd., Warley, vol. 1, p. 391
30. Suresh, S., and Ritchie, R. O., 1983, Scripta Met., 17, 575
31. Benoit, D., Namdar-Irani, R., and Tixier, R., 1981, Mater. Sci. Eng., 45, 1
32. Toplosky, J., and Ritchie, R. O., 1981, Scripta Met., 15, 905
33. Liaw, P. K., Hudak, S. J., and Donald, J. K., 1983, in ASTM STP 791, ASTM, Philadelphia, vol. 1, p. 163
34. Vasudévan, A. K., and Suresh, S., 1982, Metall. Trans., 13A, 2271
35. Lafarie-Frenot, M. C., and Gasc, C., 1983, Fat. Eng. Mat. Struct., 6, 329
36. Suresh, S., Vasudévan, A. K., and Bretz, P. E., 1984, Metall. Trans., 15A, 369
37. Carter, R. D., Lee, E. W., Starke, E. A., and Beevers, C. J., 1984, Metall. Trans., 15A, 555
38. Zaiken, E., and Ritchie, R. O., 1985, Mater. Sci. Eng., 68 in press
39. Minakawa, K., Matsuo, Y., and McEvily, A. J., 1982, Metall. Trans., 13A, 439
40. Dutta, V. B., Suresh, S., and Ritchie, R. O., 1984, Metall. Trans., 15A, 1193

41. Forsyth, P. J. E., 1962, in Crack Propagation, Proc. Cranfield Symp., Cranfield Press, p. 76
42. Gell, M., and Leverant, G. R., 1968, Acta Met., 16, 553
43. Brown, C. W., King, J. E., and Hicks, M. A., 1984, Met. Sci., 18, 374
44. Schulte, K., Nowack, H., and Trautmann, K. H., 1980, Z. Werkstofftech., 11, 287
45. Suresh, S., 1983, Metall. Trans., 14A, 2375
46. Yoder, G. R., Cooley, L. A., and Crooker, T. W., 1978, Metall. Trans., 9A, 1413
47. Gerdes, C., Gysler, A., and Lütjering, G., 1984, in Fatigue Crack Growth Threshold Concepts, D. L. Davidson and S. Suresh, eds., TMS-AIME, Warrendale, p. 465
48. Park, D. H., and Fine, M. E., 1984, in Fatigue Crack Growth Threshold Concepts, D. L. Davidson and S. Suresh, eds., TMS-AIME, Warrendale, p. 145
49. McMeeking, R. M., and Evans, A. G., 1982, J. Amer. Cer. Soc., 65, 242
50. Bilby, B. A., Cardew, G. E., and Howard, I. C., 1977, in Fracture 1977, Proc. Fourth Int. Conf. on Fracture (ICF-4), D. M. R. Taplin, ed., Pergamon Press, Oxford, vol. 3, p. 197
51. Ritchie, R. O., 1982, in Fatigue Thresholds, Proc. First Int. Conf. on Fatigue Thresholds, J. Bäcklund, A. Blom, and C. J. Beevers, eds., EMAS Ltd., Warley, vol. 1, p. 503

52. Esaklul, K. A., Wright, A. G., and Gerberich, W. W., 1984, in Fatigue Crack Growth Threshold Concepts, D. L. Davidson and S. Suresh, eds., TMS-AIME, Warrendale, p. 299
53. Suresh, S., and Ritchie, R. O., 1982, Met. Sci., 16, 529
54. Pendse, R. D., and Ritchie, R. O., 1985, Metall. Trans., 16A, in review
55. Ritchie, R. O., 1977, Met. Sci., 11, 368
56. Wasynczuk, J., Ritchie, R. O., and Thomas, G., 1984, Mater. Sci. Eng., 62, 79
57. Tzou, J.-L., 1984, unpublished work, University of California, Berkeley
58. Hornbogen, E., and Zum Gahr, K. H., 1976, Acta Met., 24, 581
59. Antolovich, S. D., and Campbell, J. E., 1982, in Application of Fracture Mechanics for Selection of Metallic Structural Materials, J. E. Campbell, W. W. Gerberich, and J. H. Underwood, eds., ASM, Metals Park, p. 253
60. Balmuth, E. S., and Schmidt, R., 1981, in Aluminum-Lithium Alloys, T. H. Sanders and E. A. Starke, eds., TMS-AIME, Warrendale, p. 69
61. Döker, H., Bachmann, V., and Marci, G., 1982, in Fatigue Thresholds, Proc. First Int. Conf. on Fatigue Thresholds, J. Bäcklund, A. Blom, and C. J. Beevers, eds., EMAS Ltd., Warley, vol. 1, p. 45
62. Newman, J. C., 1983, in Behaviour of Short Cracks in Airframe Components, AGARD Conf. Proc. No. 328, AGARD, France, p. 6.1

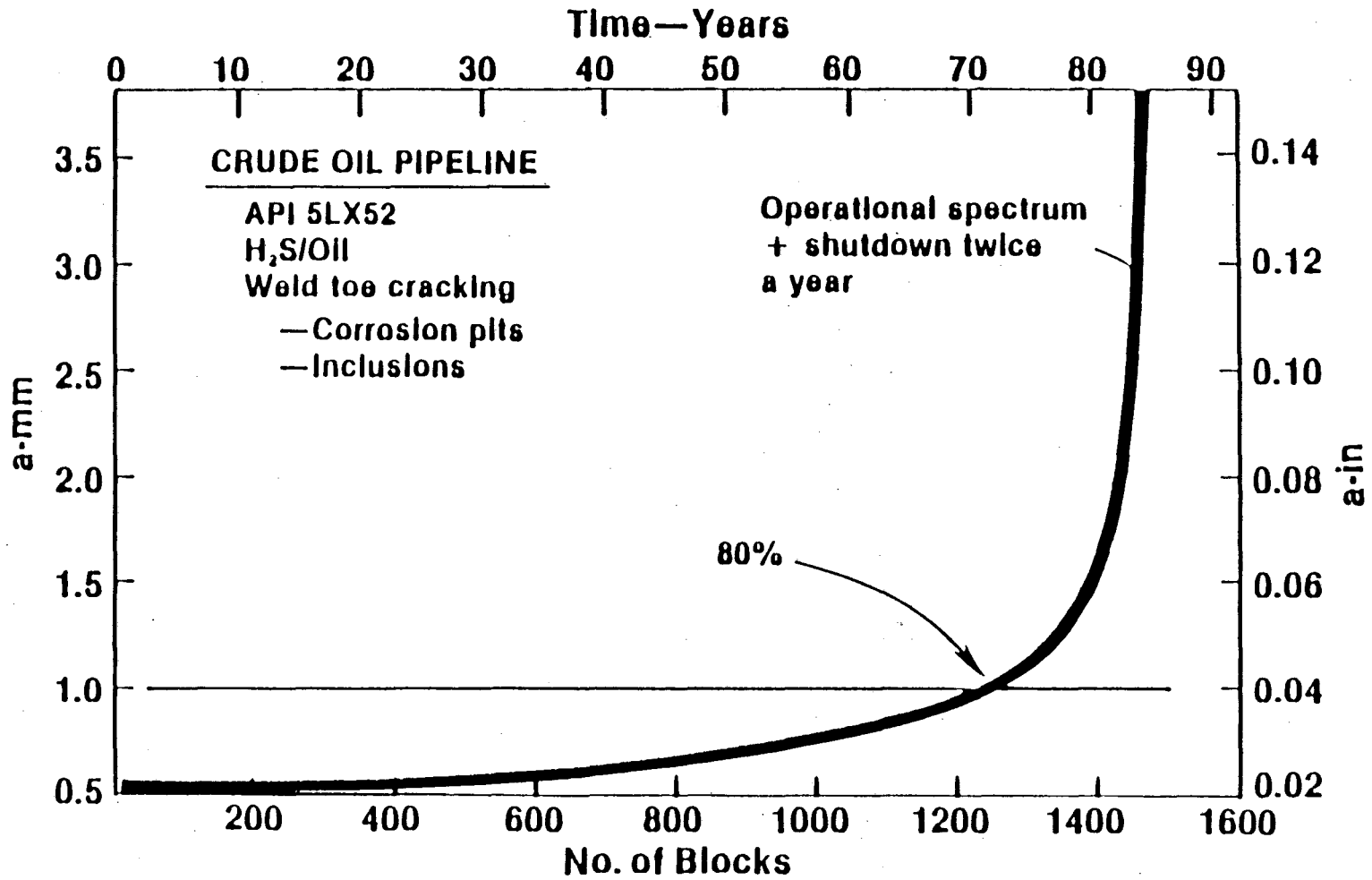
63. Cadman, A. J., Brook, R., and Nicholson, C. E., 1982, in Fatigue Thresholds, Proc. First Int. Conf. on Fatigue Thresholds, J. Bäcklund, A. Blom, and C. J. Beevers, eds., EMAS Ltd., Warley, vol. 1, p. 59
64. Duggan, T. V., 1982, in Fatigue Thresholds, Proc. First Int. Conf. on Fatigue Thresholds, J. Bäcklund, A. Blom, and C. J. Beevers, eds., EMAS Ltd., Warley, vol. 2, p. 809
65. Breat, J. L., Mudry, F., and Pineau, A., 1983, Fat. Eng. Mat. Struct., 6, 349
66. Minakawa, K., Newman, J. C., and McEvily, A. J., 1983, Fat. Eng. Mat. Struct., 6, 359
67. Zaiken, E., and Ritchie, R. O., 1984, Scripta Met., 18, 847
68. Zaiken, E., and Ritchie, R. O., 1985, Metall. Trans., 16A, in review
69. James, M. N., and Knott, J. F., 1985, Fat. Eng. Mat. Struct., 8, in review
70. Zaiken, E., and Ritchie, R. O., 1985, Eng. Fract. Mech., 21, in press
71. Ritchie, R. O., Zaiken, E., and Blom, A. F., 1984, in Fundamental Questions and Critical Experiments on Fatigue, ASTM STP, ASTM, Philadelphia, in review
72. Au, P., Topper, T. H., and El Haddad, M. L., 1983, in Behavior of Short Cracks in Airframe Components, AGARD Conf. Proc. No. 328, AGARD, France, p. 11.1

73. Marissen, R., Trautmann, K. H., and Nowack, H., 1984, Eng. Fract. Mech., 19, 863
74. Suresh, S., and Vasudévan, A. K., 1984, in Fatigue Crack Growth Threshold Concepts, D. L. Davidson and S. Suresh, eds., TMS-AIME, Warrendale, p. 361
75. James, M. R., and Morris, W. L., 1983, Metall. Trans., 14A, 153
76. Beevers, C. J., Bell, K., Carlson, R. L., and Starke, E. A., 1984, Eng. Fract. Mech., 19, 93
77. Gerberich, W. W., Yu, W., and Esaklul, K., 1984, Metall. Trans., 15A, 875
78. Horng, J. L., and Fine, M. E., 1984, in Fatigue Crack Growth Threshold Concepts, D. L. Davidson and S. Suresh, eds., TMS-AIME, Warrendale, p. 115
79. Ritchie, R. O., and Suresh, S., 1983, Mater. Sci. Eng., 57, L27



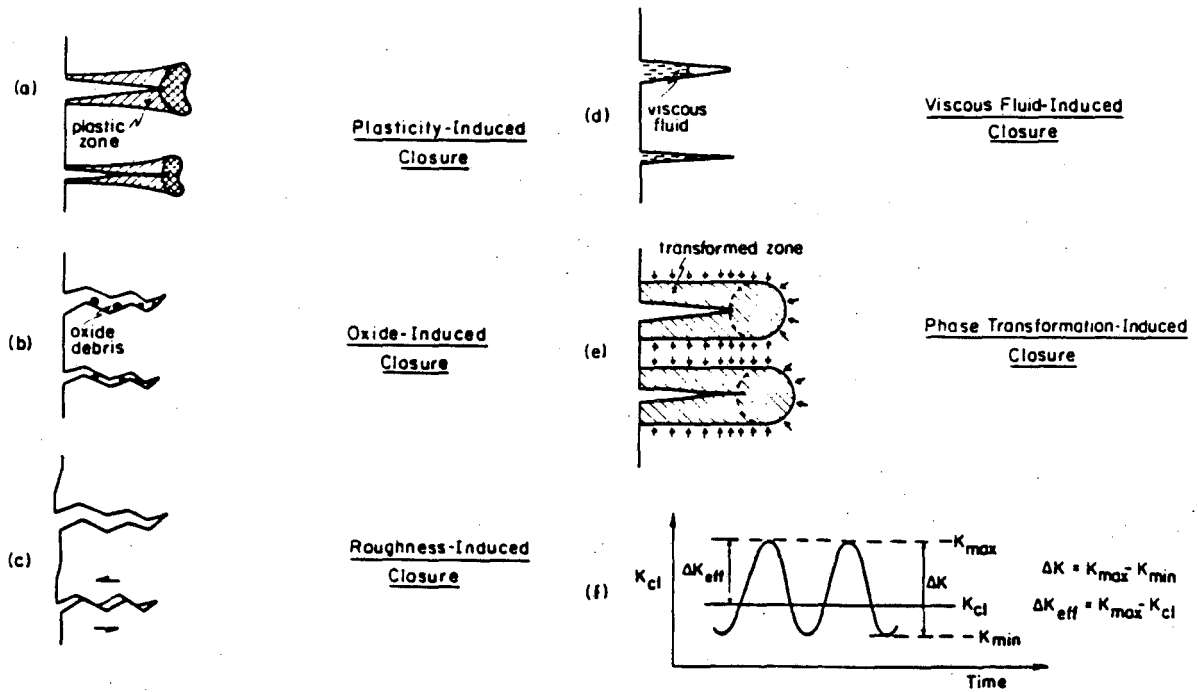
XBL 835-9687

Fig. 1. Schematic variation of da/dN with ΔK for short and long fatigue cracks.



XBL 841-524

Fig. 2. Defect-tolerant fatigue life predictions for a sour gas pipeline (11).

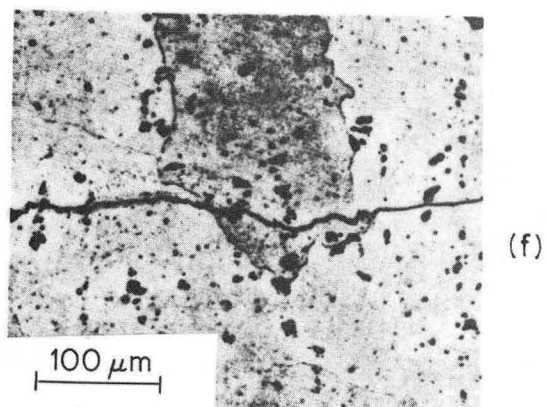
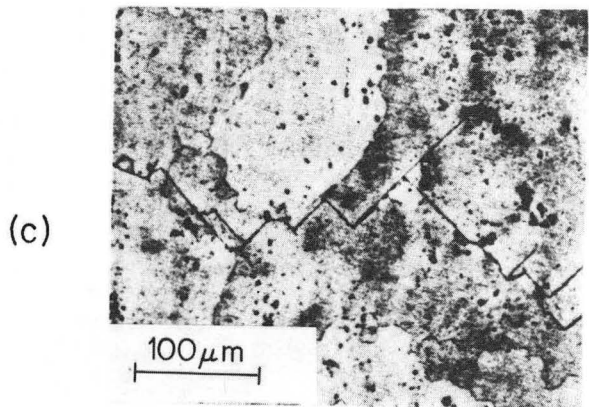
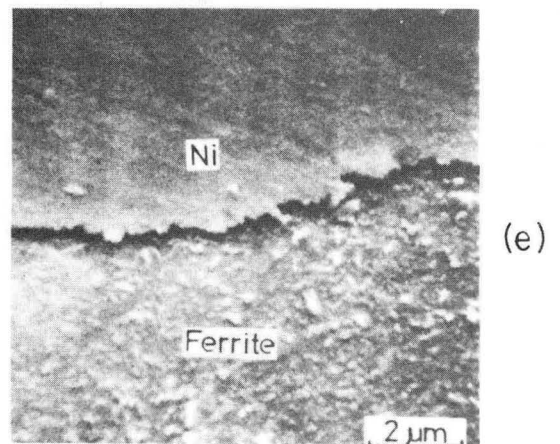
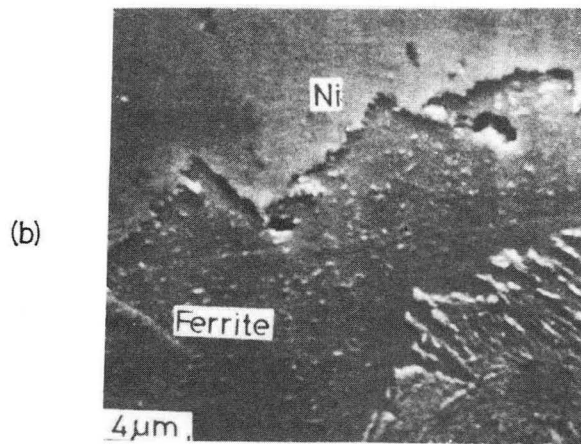
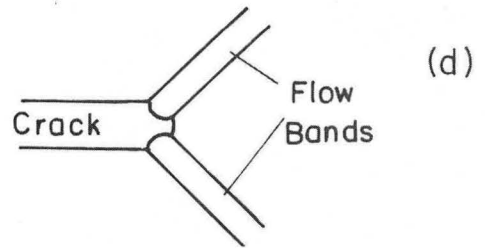
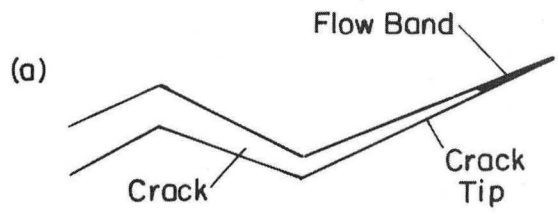


XBL 839-6312A

Fig. 3. Schematic illustration of primary mechanisms of fatigue crack closure.

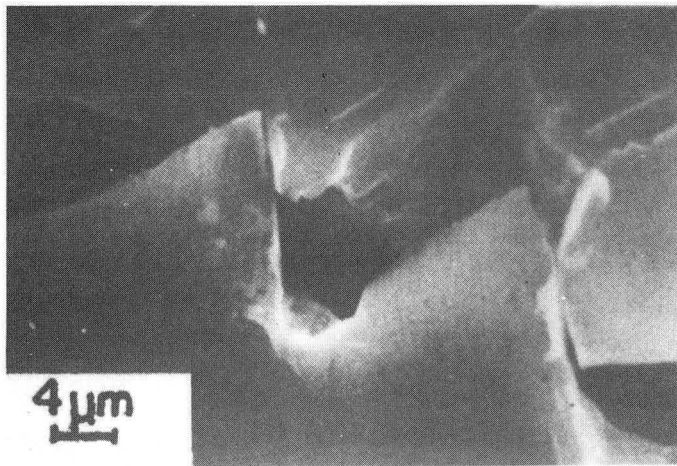
Near-Threshold: $r_y < d_g$
(Stage I, Modes II+I)

Higher Growth Rates: $r_y > d_g$
(Stage II, Mode I)



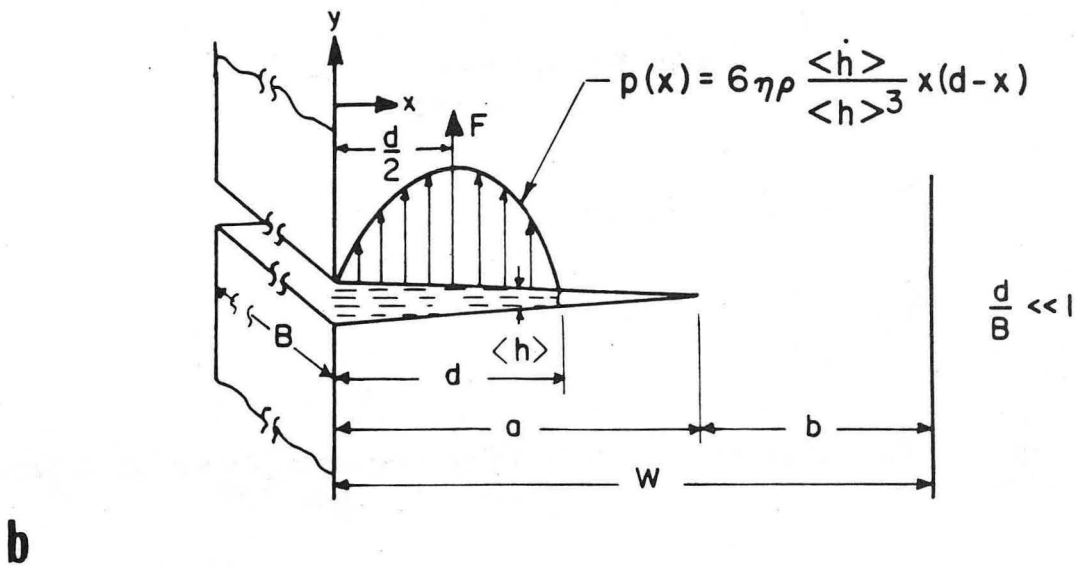
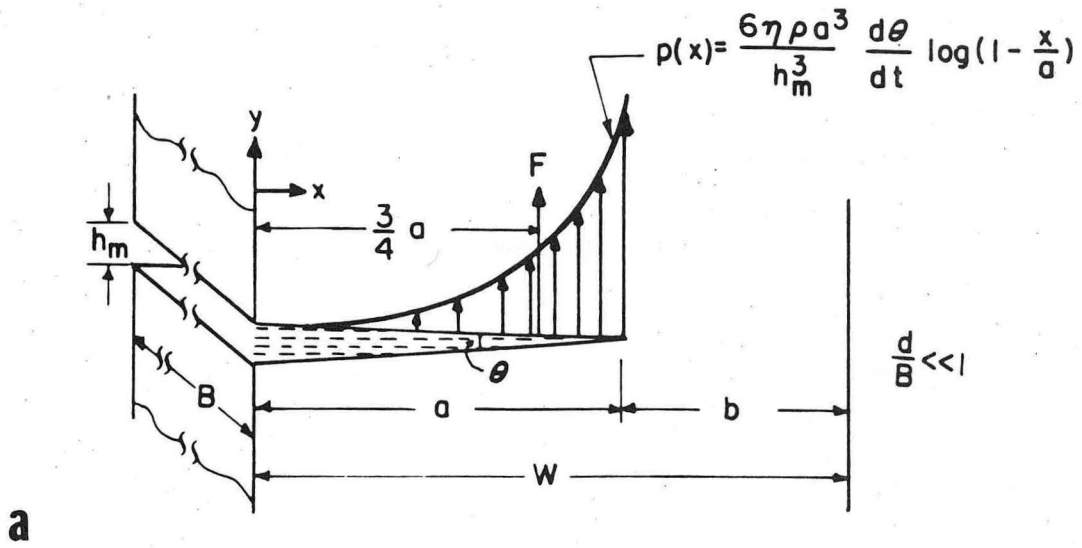
XBB 821-736

Fig. 4. Crack path profiles at near-threshold at higher growth rates (12).



XBB 820-9876A

Fig. 5. Asperity contact during fatigue of underaged X-7075 aluminum alloy (45).



XBL 834-5537A

Fig. 6. Internal fluid-induced pressure distributions for a) completely filled and b) partially filled cracks (25).

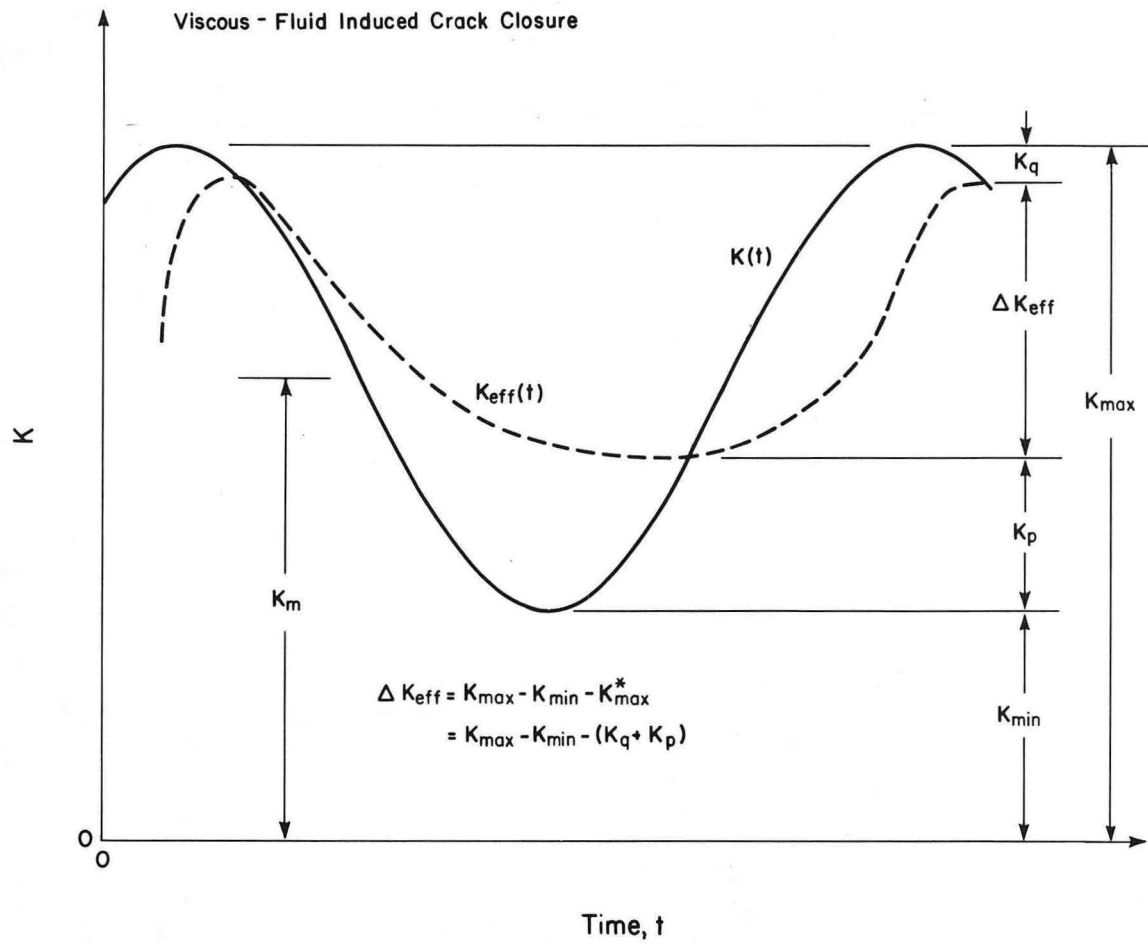
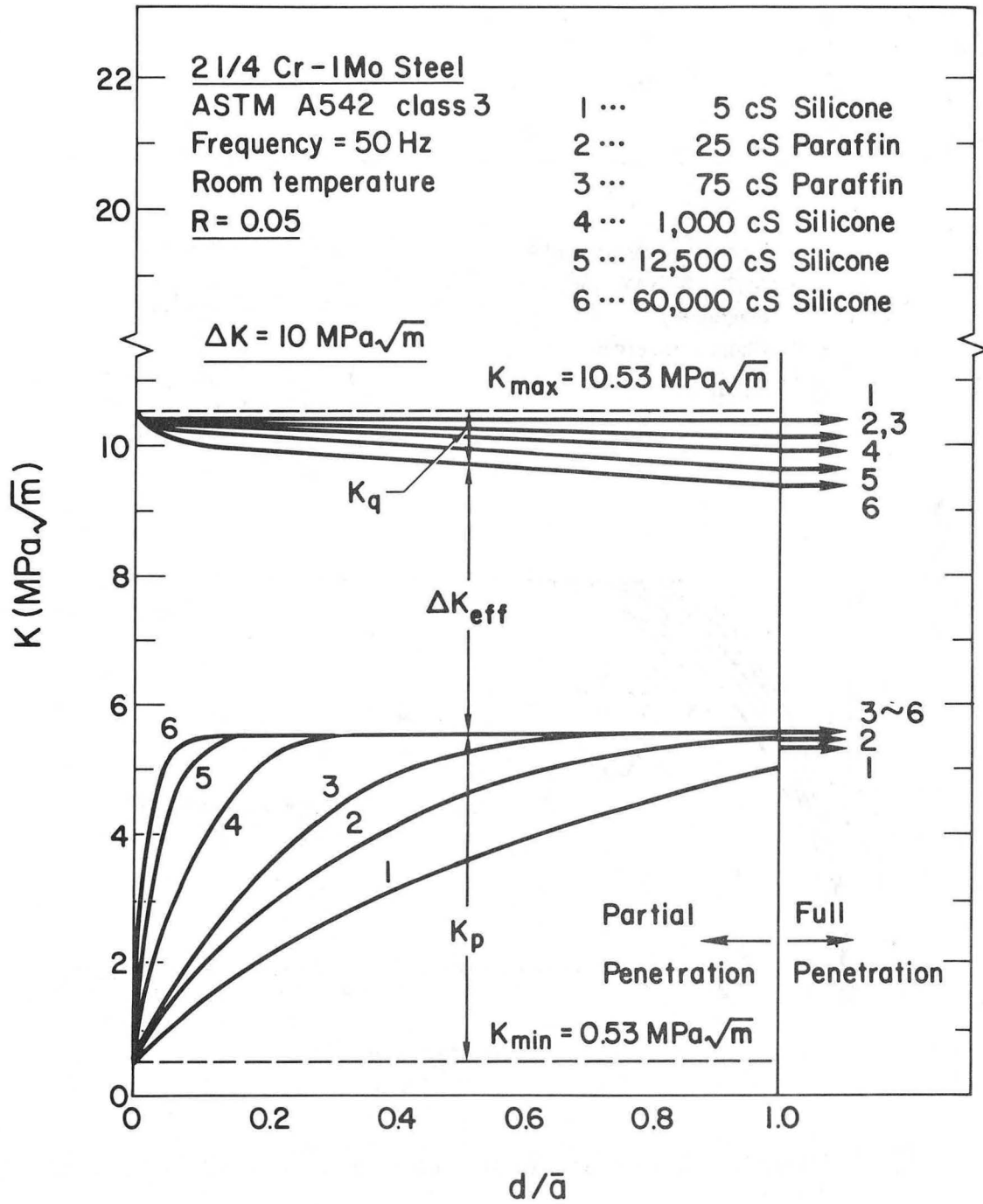
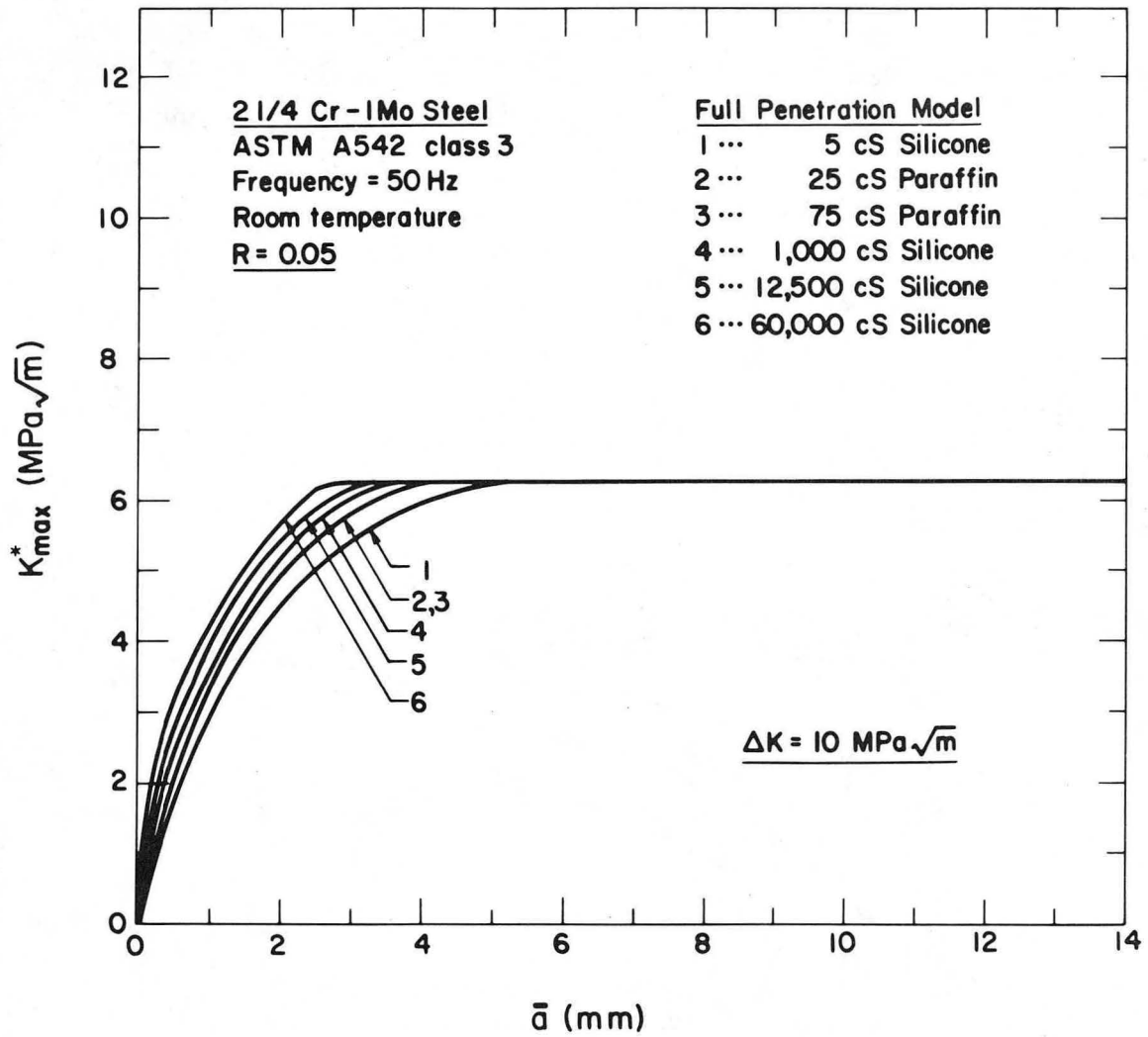


Fig. 7. Variation in cyclic K_I incorporating fluid-induced closure (25).



XBL 841-6733A

Fig. 8. Predictions of ΔK_{eff} with fluid penetration d for oils of varying viscosity (25).



XBL 841-6735A

Fig. 9. Predicted variation of closure K_{max}^* with crack length a (25).

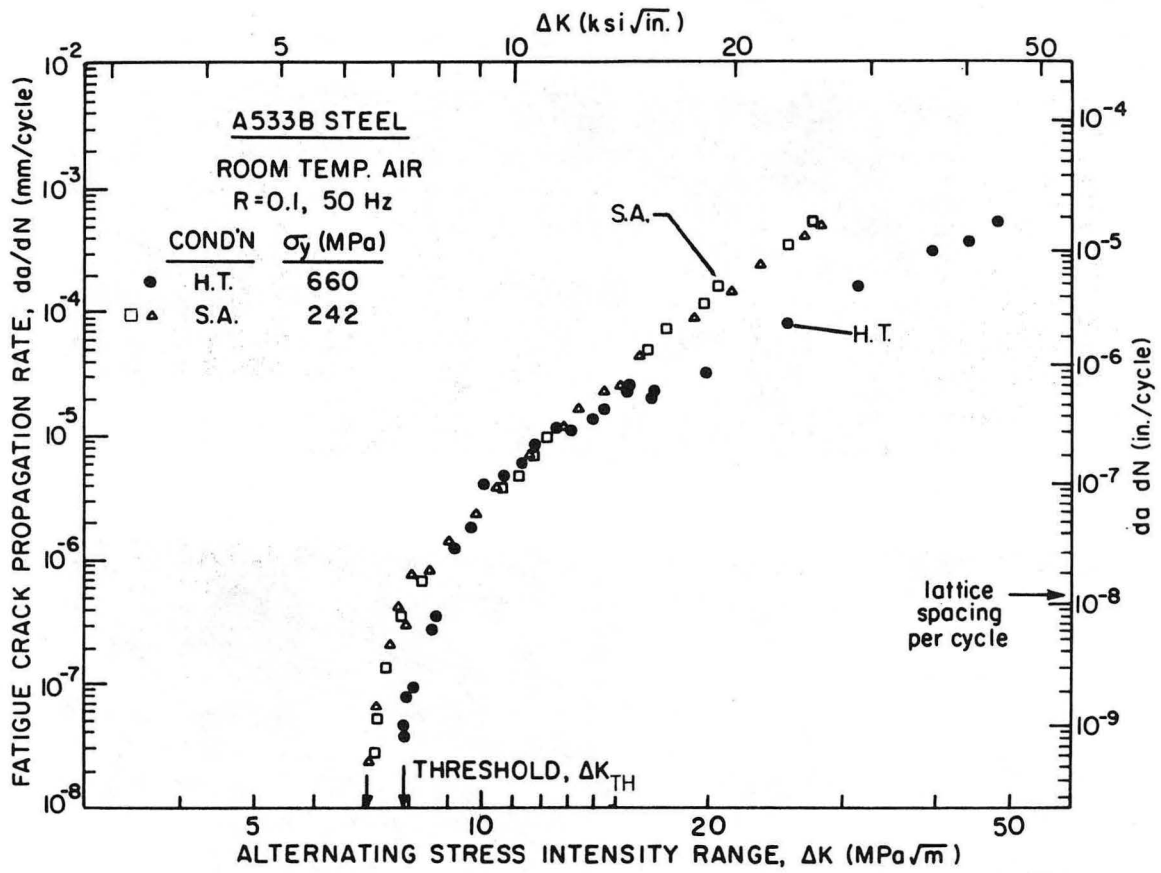
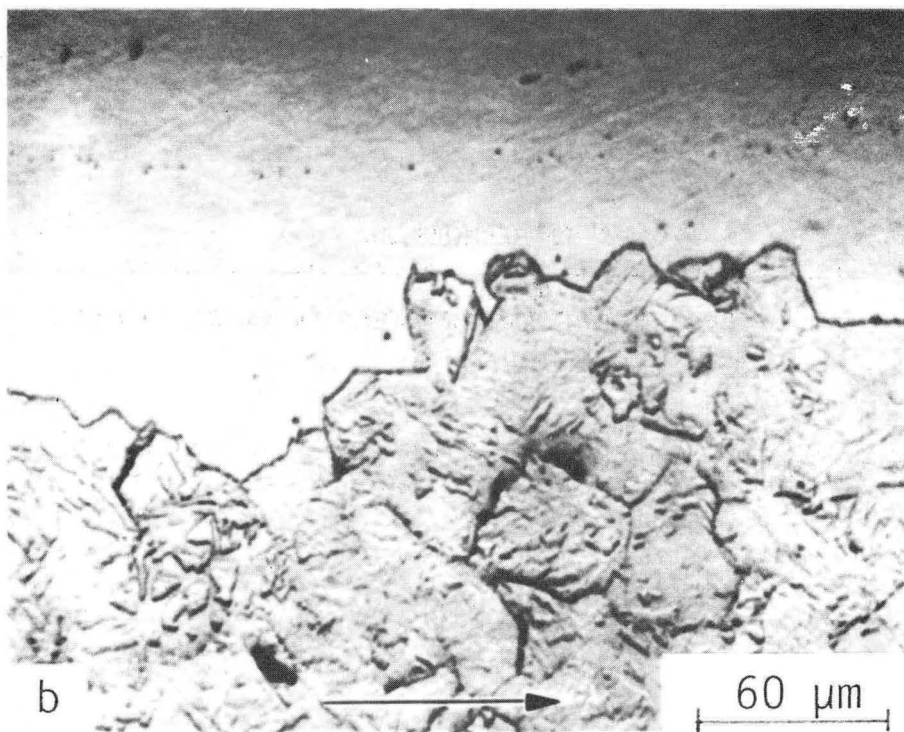
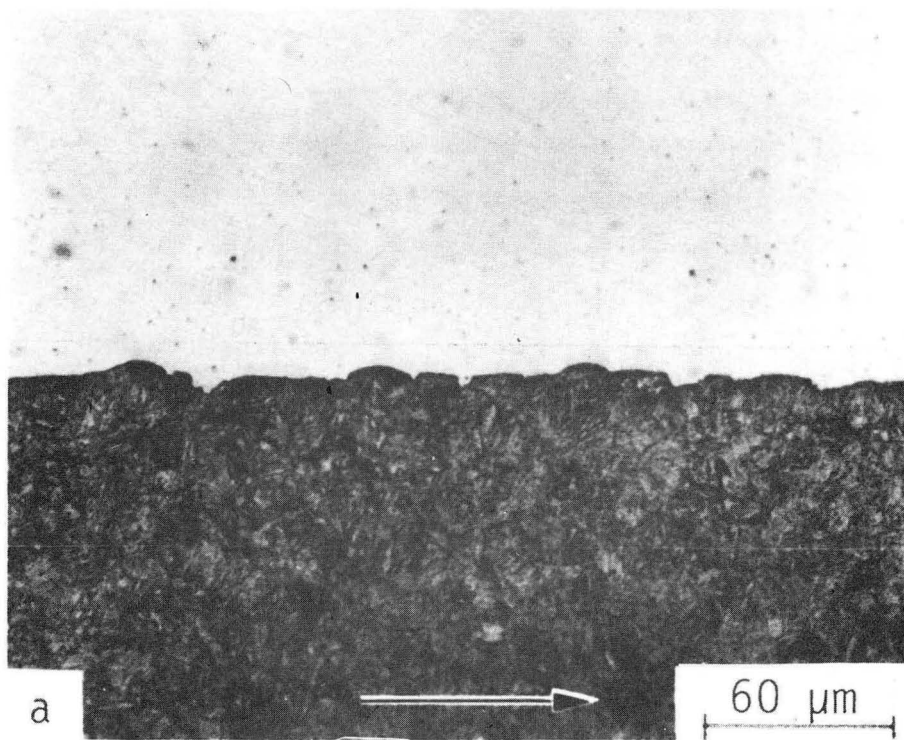
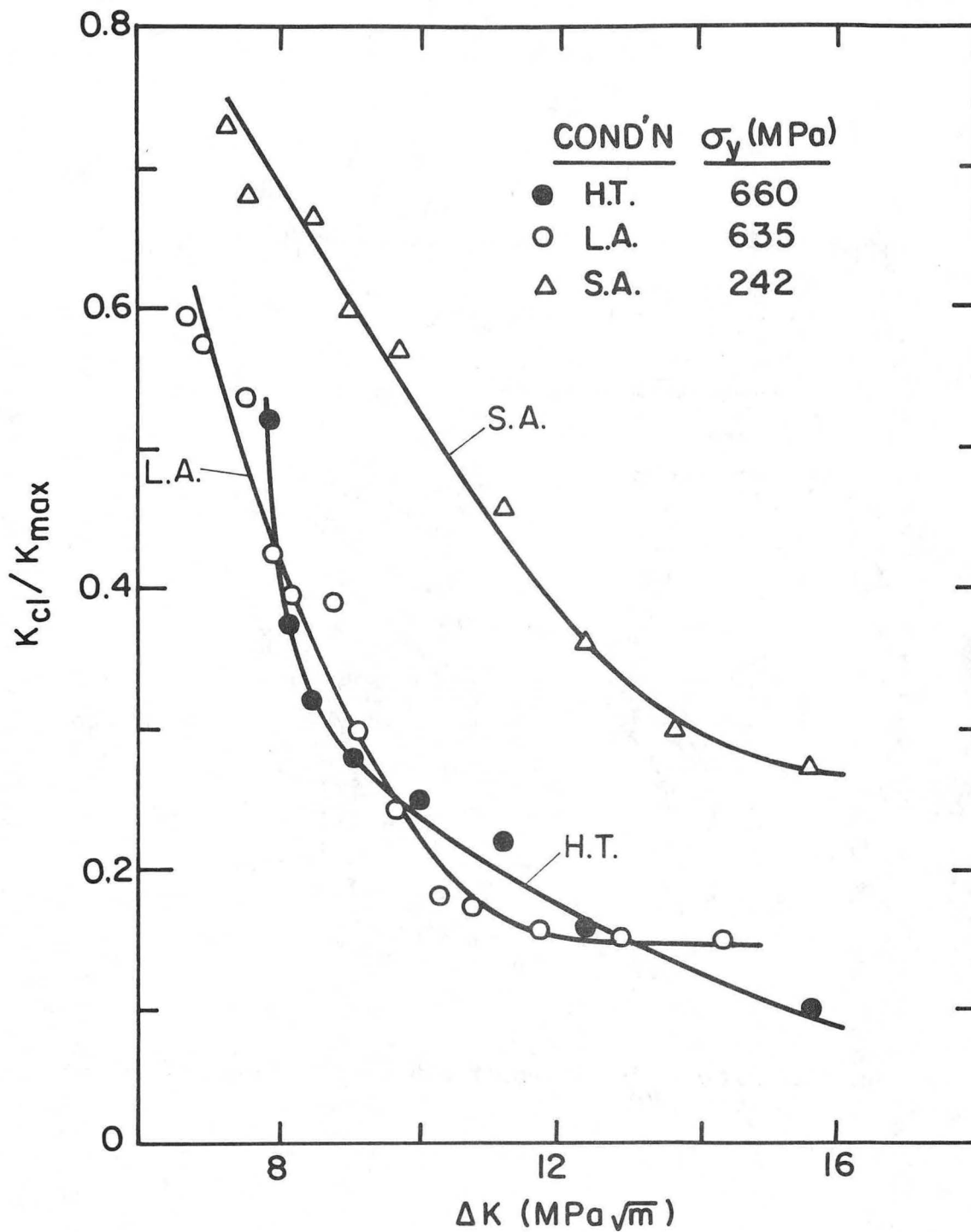


Fig. 10. Crack propagation in unattacked (HT) and prior hydrogen attack (SA) A533B steel (54).



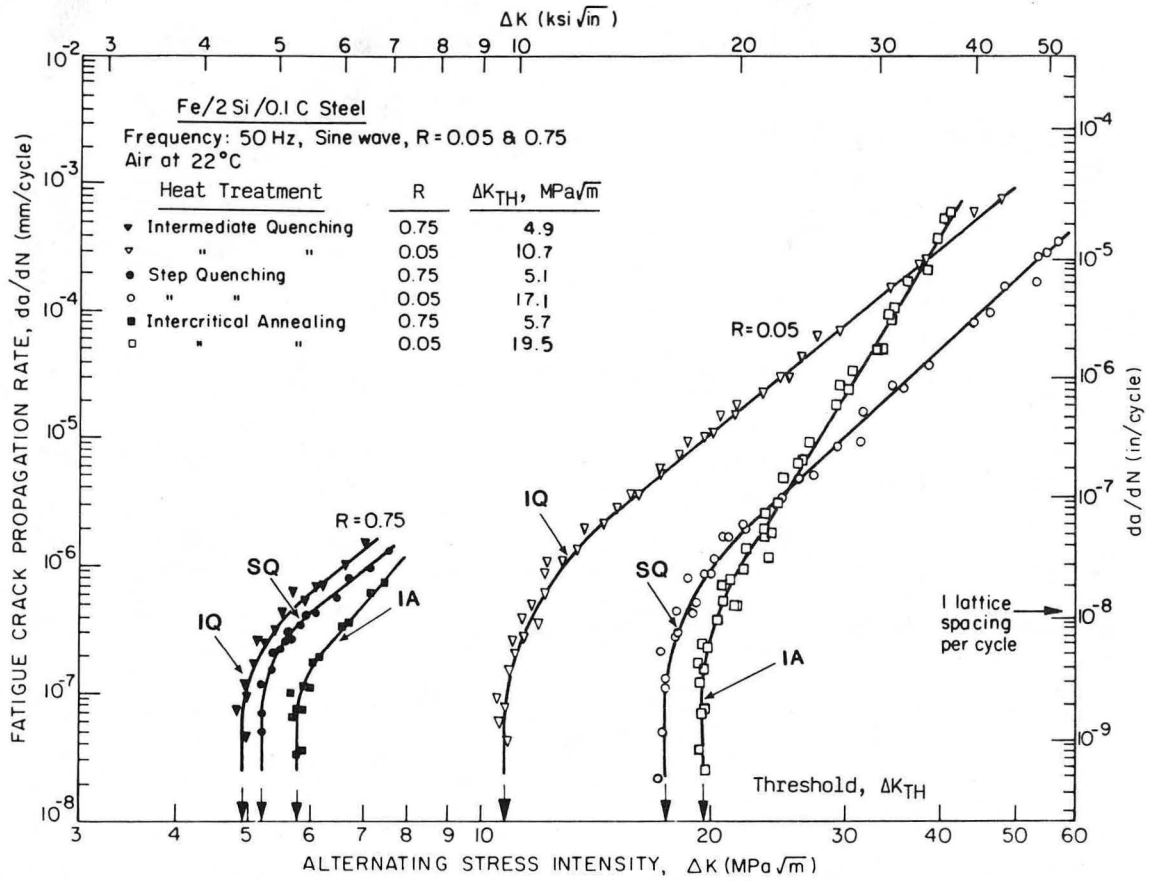
XBB 844-3299A

Fig. 11. Crack path profiles in a) unattacked and b) prior hydrogen attacked A533B steel (54).



XBL 845-6962A

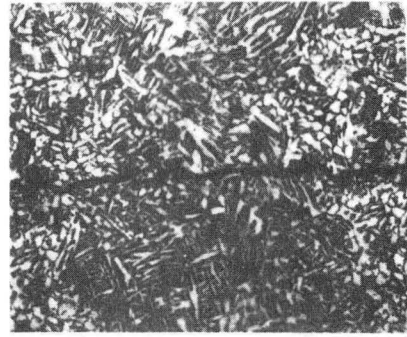
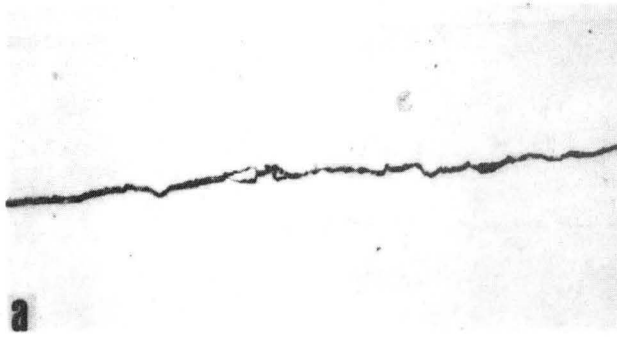
Fig. 12. Closure measured in unexposed and prior hydrogen exposed A533B steel (54).



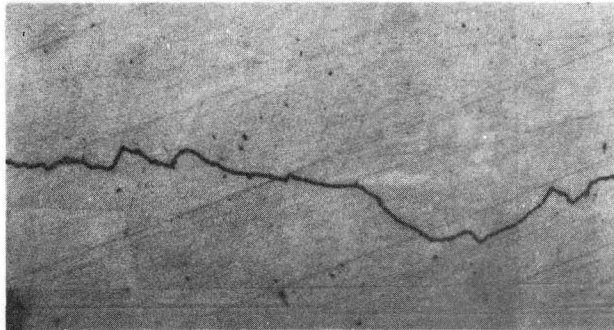
XBL 838-10897A

Fig. 13. Fatigue crack growth behavior in Fe-2Si-0.1C dual-phase steel (40).

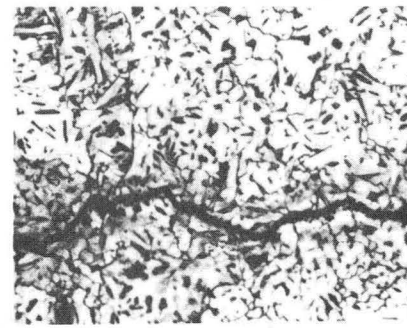
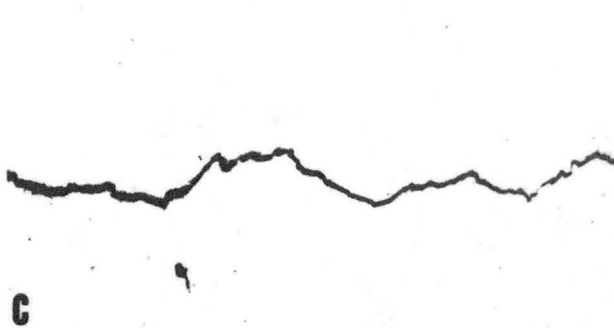
INTERMEDIATE QUENCHING (IQ)



STEP QUENCHING (SQ)



INTERCRITICAL ANNEALING (IA)

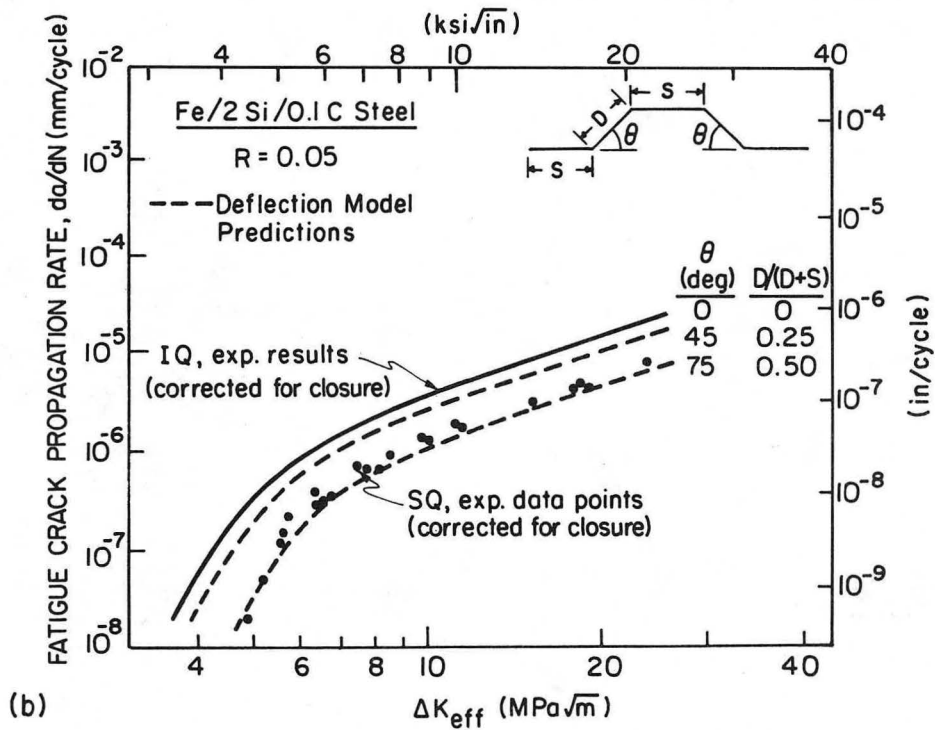
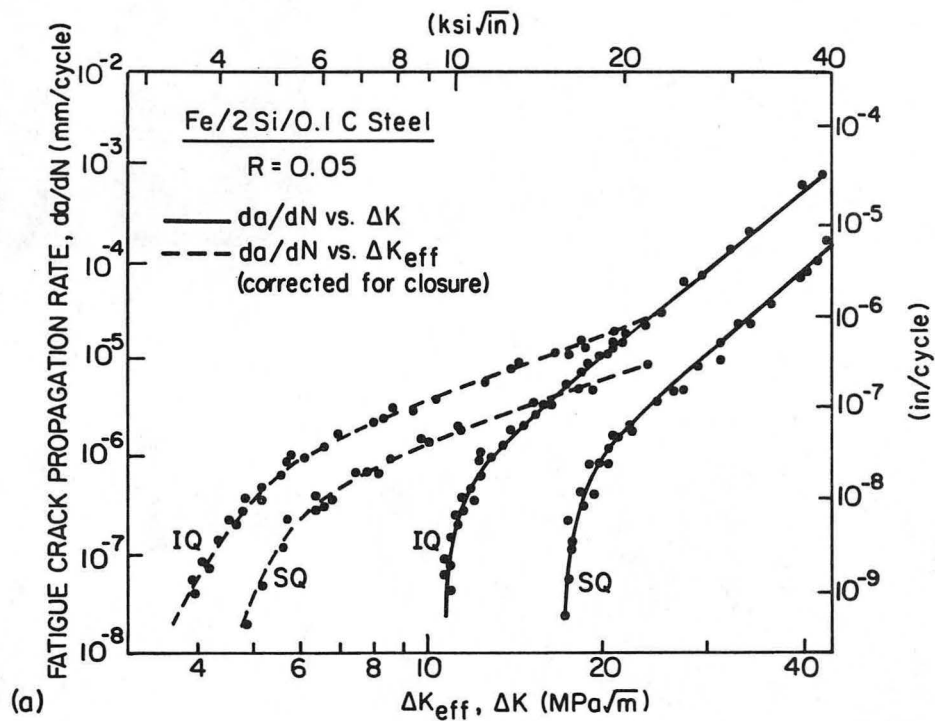


250 μm

Crack Growth Direction
→

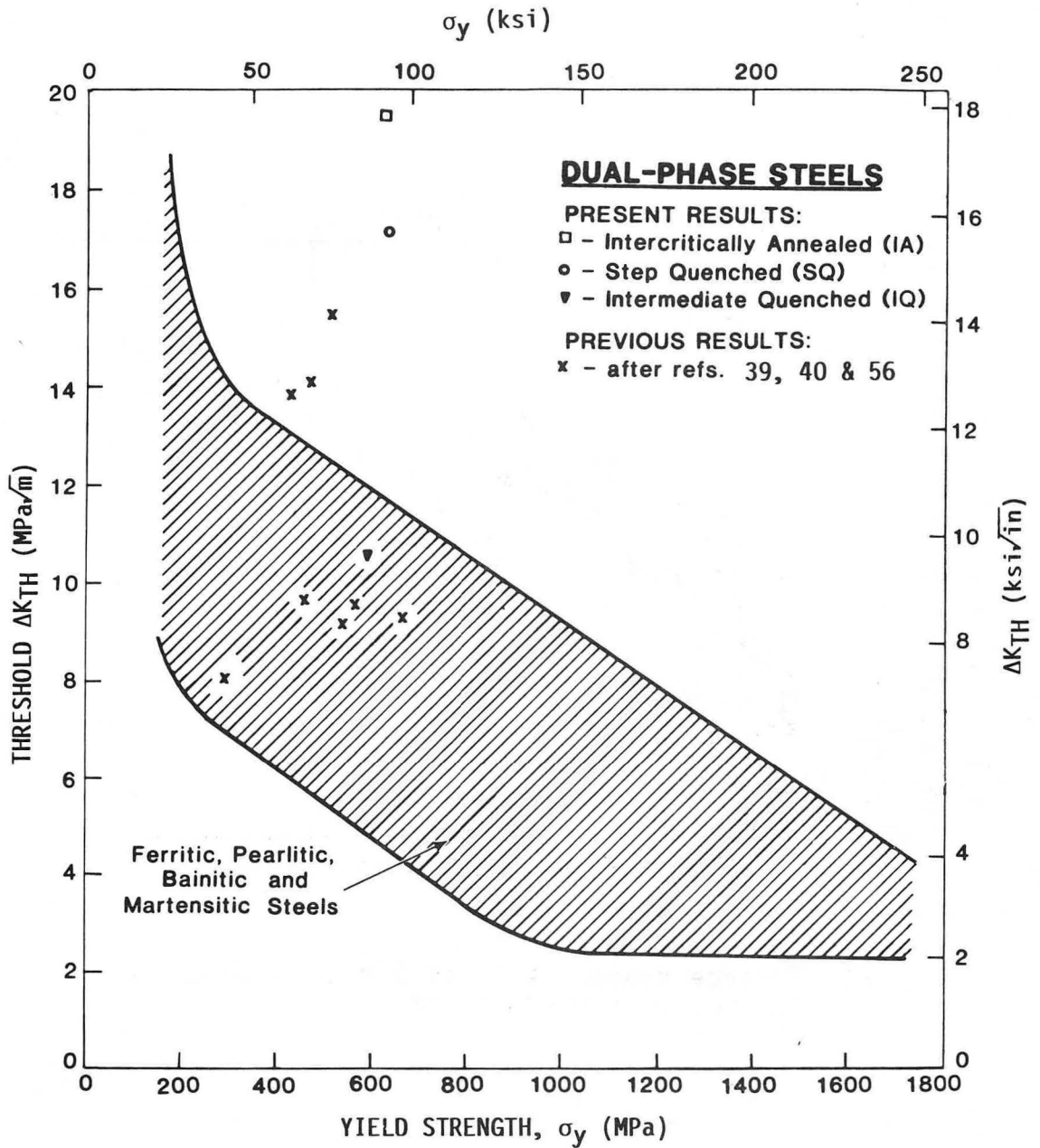
XBB 839-7928

Fig. 14. Fatigue crack growth profiles in Fe-2Si-0.1C dual-phase steel (40).



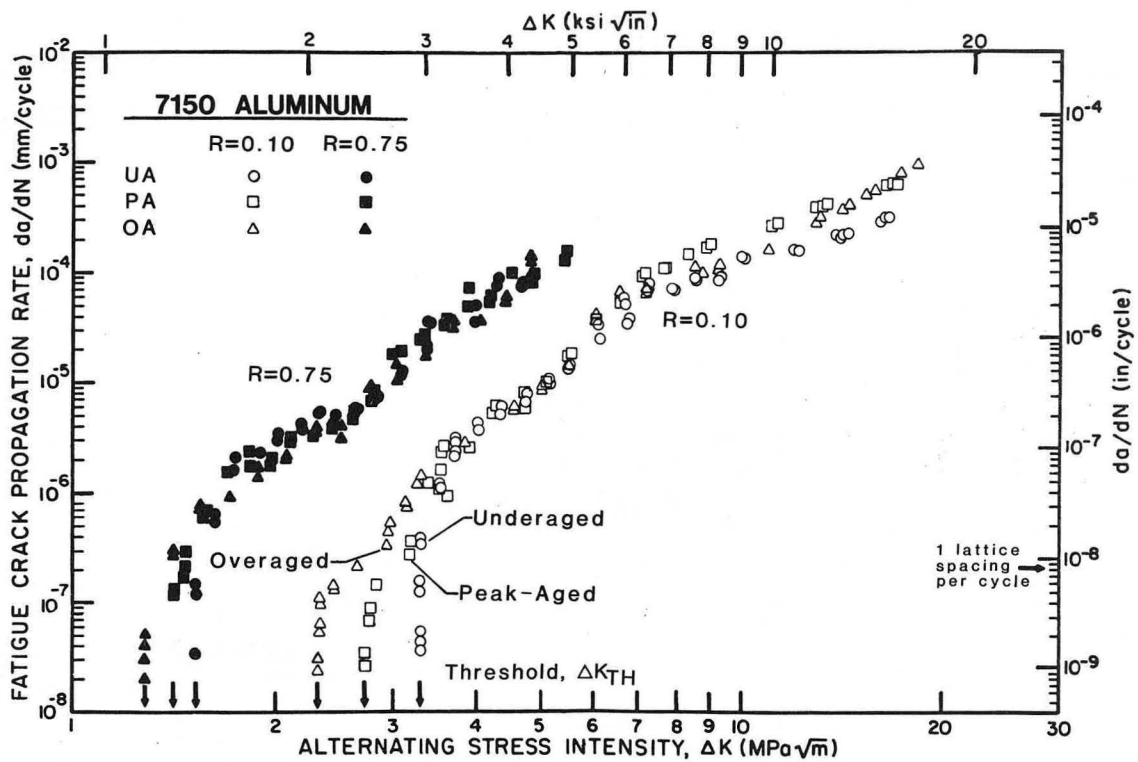
XBL 839-6311

Fig. 15. Estimated contributions from crack closure and crack deflection in dual-phase steel (40).



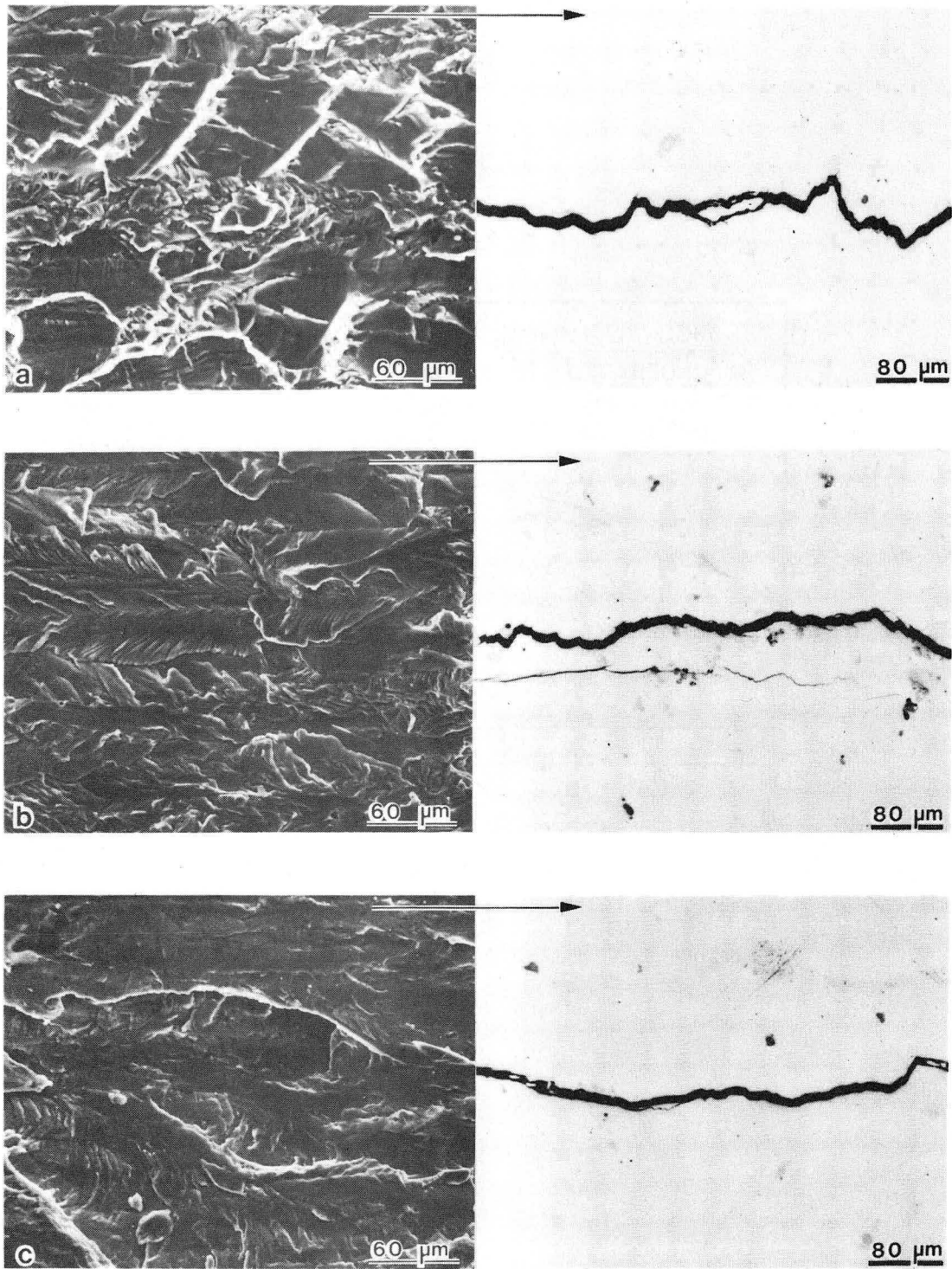
XBL 838-10895B

Fig. 16. Variation of ΔK_{TH} with yield strength showing exceptionally high thresholds in dual-phase steels (40).



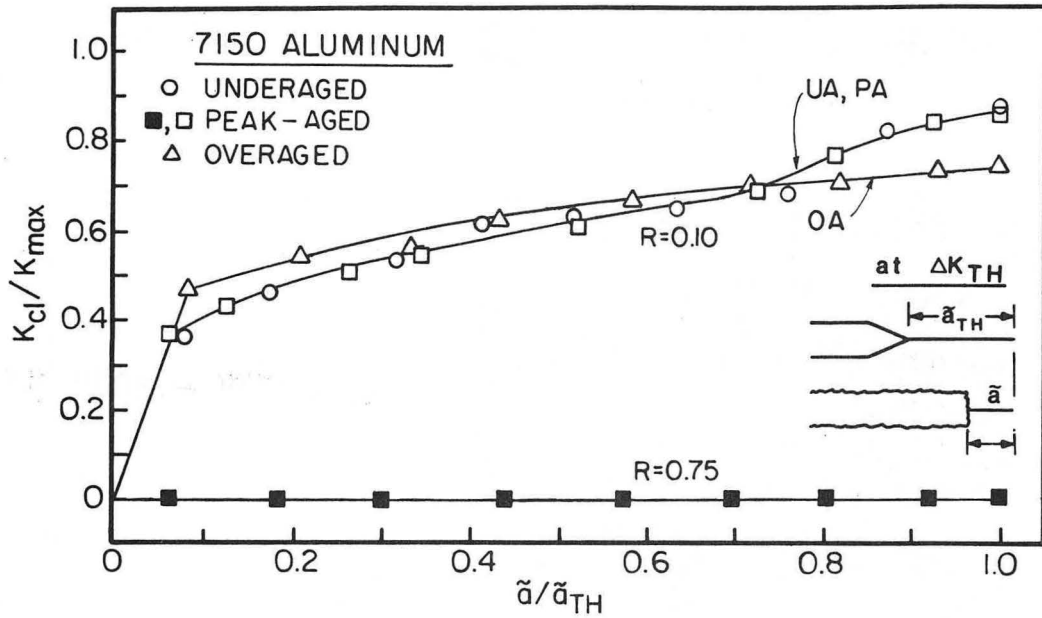
XBL 845-1801

Fig. 17. Fatigue crack growth in I/M 7150 aluminum alloy as a function of aging treatment (38).



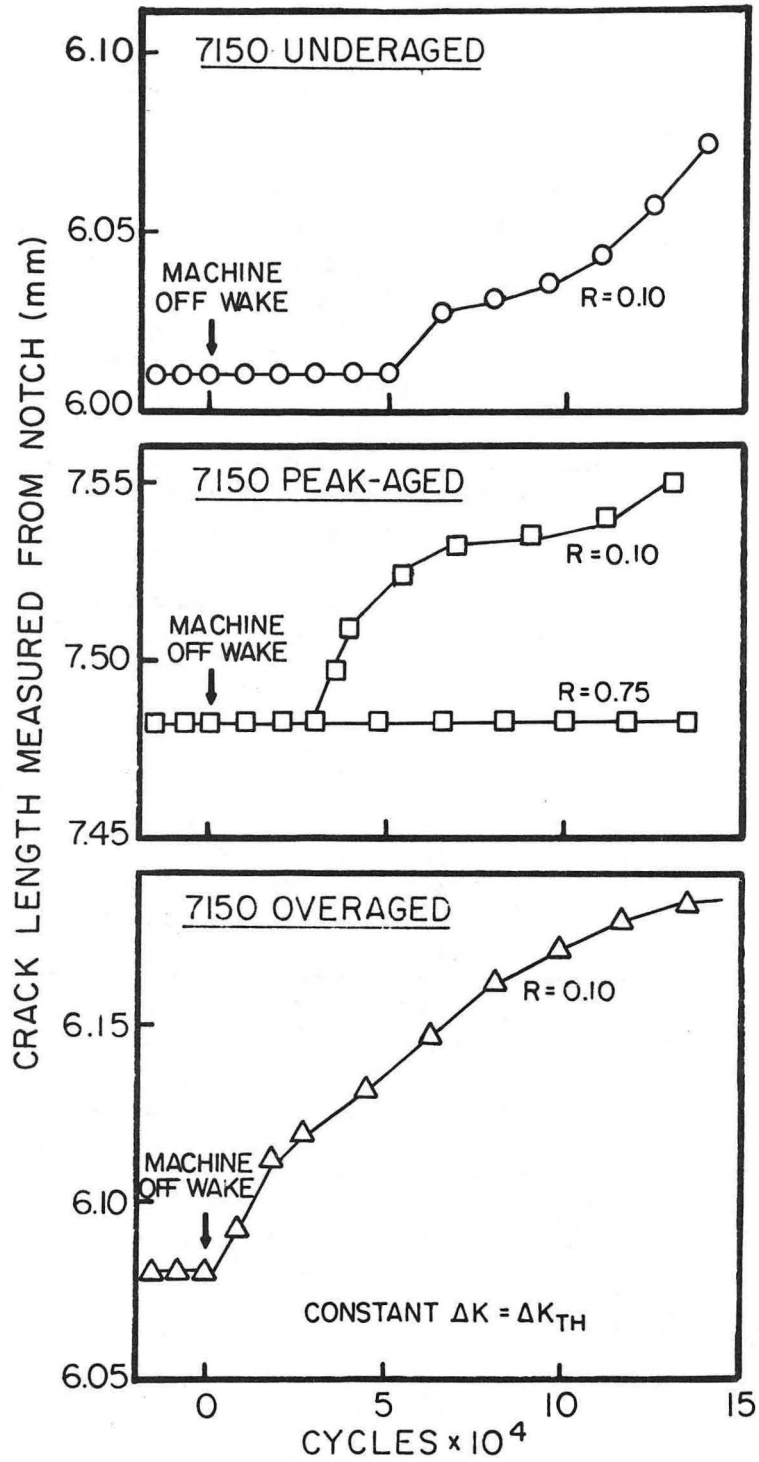
XBB 846-4328A

Fig. 18. Fatigue crack profiles for a) underaged, b) peak aged and c) overaged 7150 aluminum alloy (38).



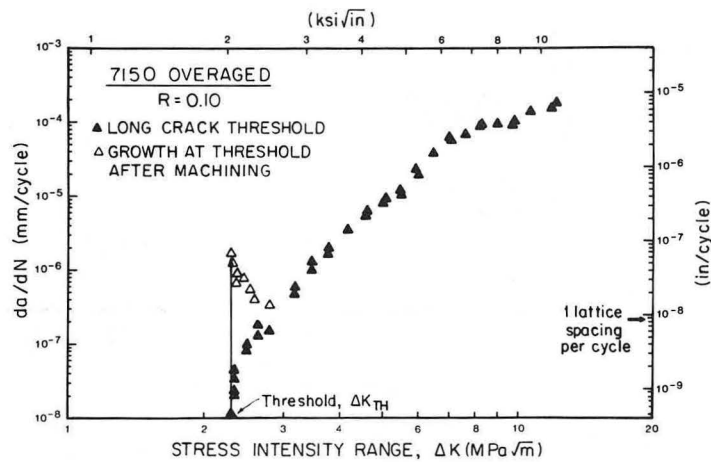
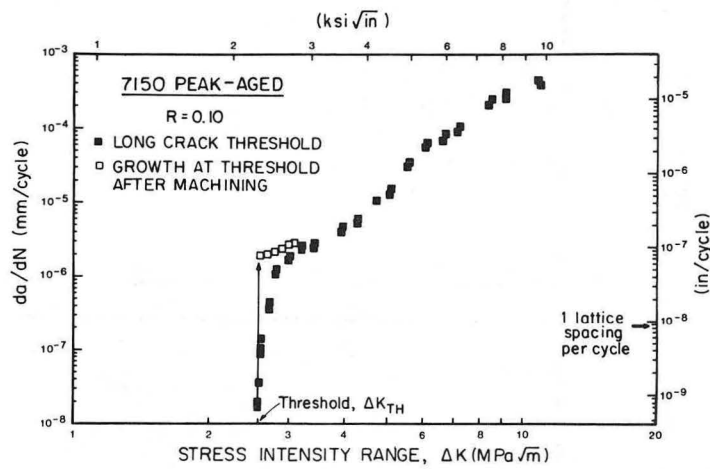
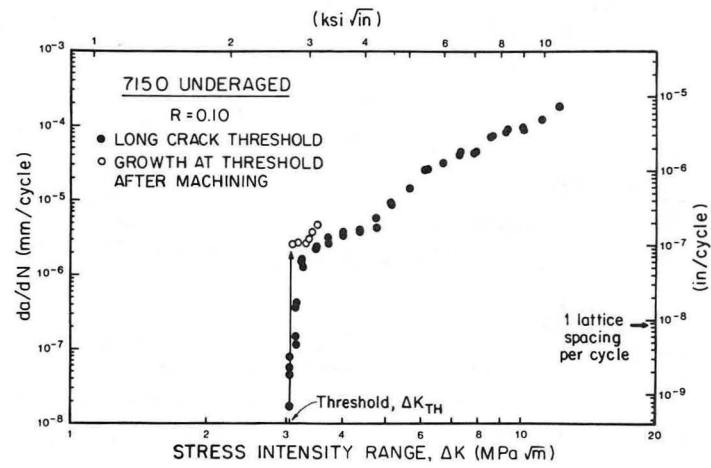
XBL 846-2433

Fig. 19. Distribution of closure along crack length at ΔK_{TH} in 7150 aluminum, estimated during wake machining experiments (67).



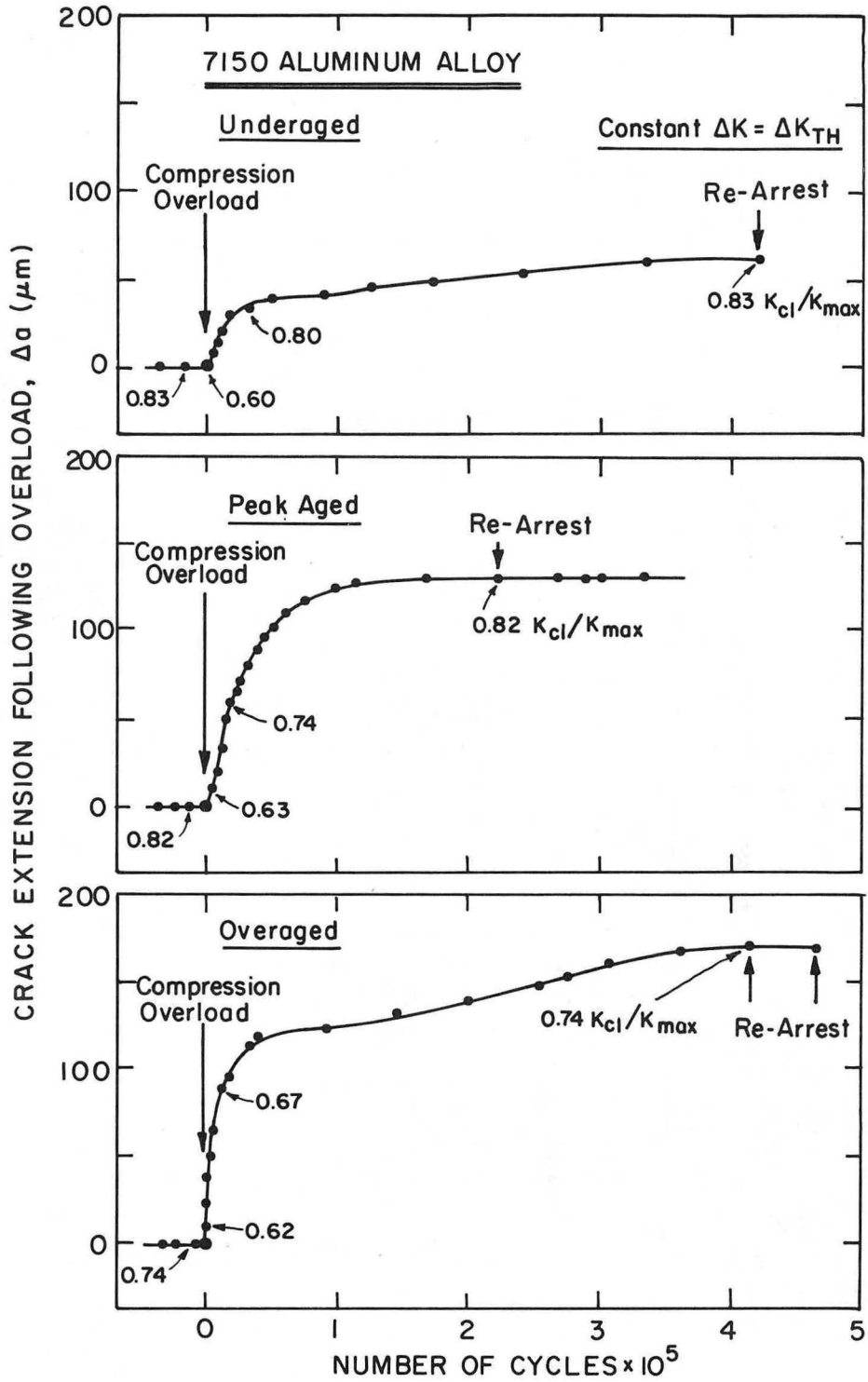
XBL 846-2434

Fig. 20. Crack growth behavior at ΔK_{TH} following wake machining in 7150 aluminum (67).



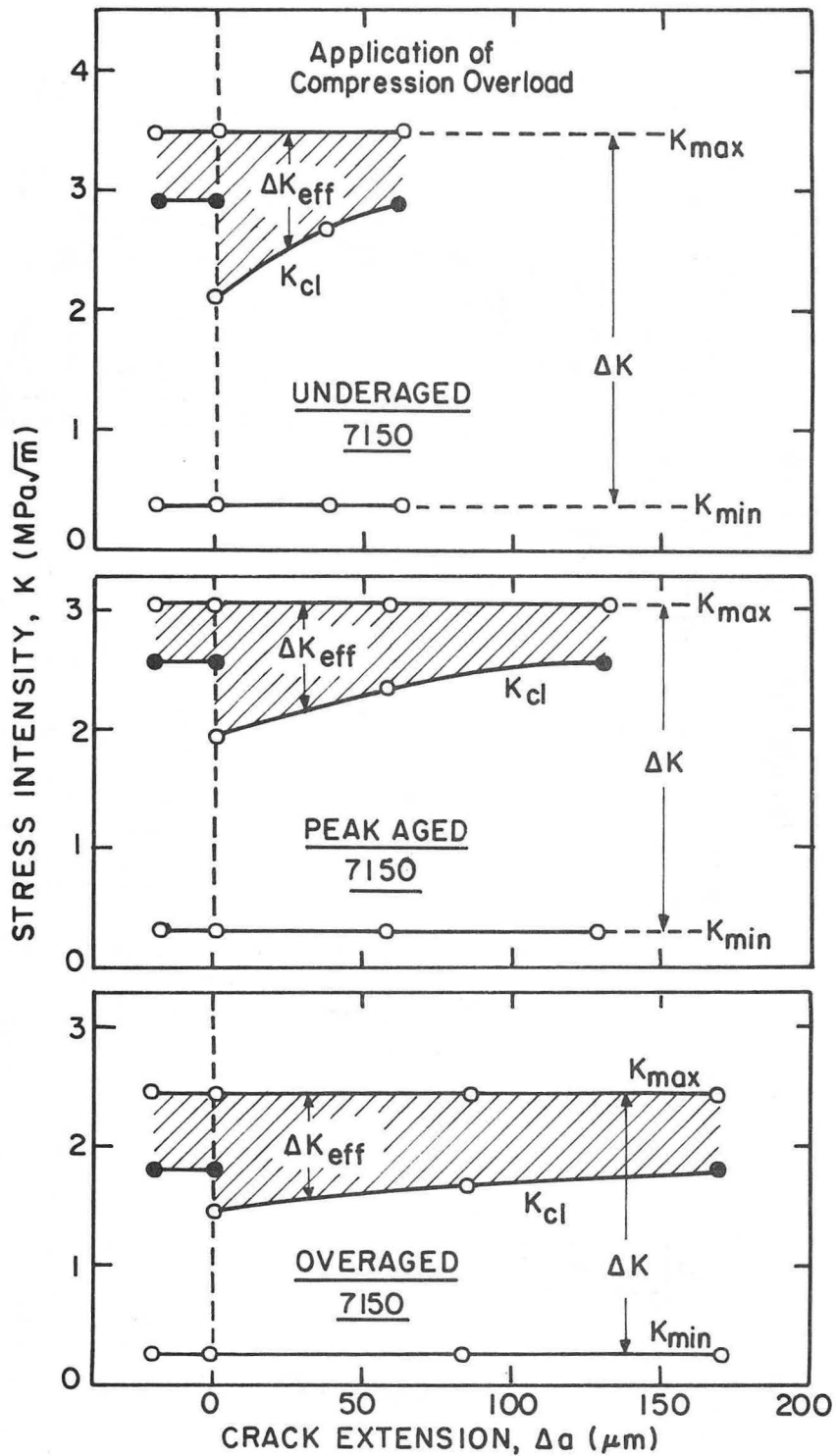
XBL 846-2435A

Fig. 21. Data for Fig. 20 plotted in terms of da/dN versus ΔK (67).



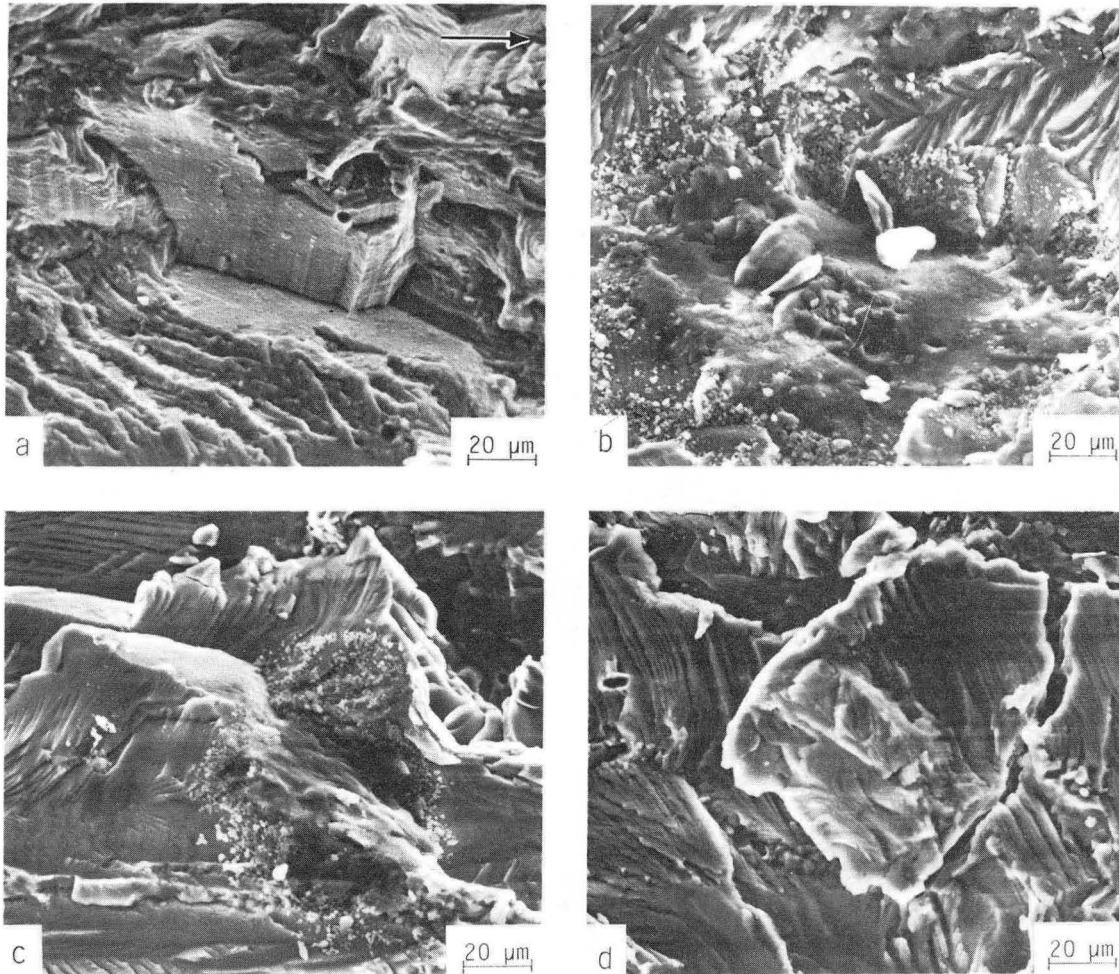
XBL 848-3409

Fig. 22. Crack growth at ΔK_{TH} following 500% compression overload (69).



XBL 848-3408

Fig. 23. Computed variation in ΔK_{eff} before and after application of compression overload (69).



XBB 848-5960

Fig. 24. Fractography of 7150 aluminum alloy at ΔK_{TH} before (a) and following compression overload, showing b) compacted fretting oxide debris, and c), d) crushed and cracked asperities (69).

This report was done with support from the Department of Energy. Any conclusions or opinions expressed in this report represent solely those of the author(s) and not necessarily those of The Regents of the University of California, the Lawrence Berkeley Laboratory or the Department of Energy.

Reference to a company or product name does not imply approval or recommendation of the product by the University of California or the U.S. Department of Energy to the exclusion of others that may be suitable.

TECHNICAL INFORMATION DEPARTMENT
LAWRENCE BERKELEY LABORATORY
UNIVERSITY OF CALIFORNIA
BERKELEY, CALIFORNIA 94720